SCIENTIFIC Publishing Limited

Prevention and Treatment of Natural Disasters

https://ojs.ukscip.com/index.php/ptnd

Article

Overview of Fault Zones Based on Remote Sensing Data as Contribution to the Safety of Infrastructure and Land Use in Southern Egypt

Barbara Theilen-Willige *

Waldstrasse 11, Scharbeutz, 23683, Germany

* Correspondence: Barbara.Theilen-Willige@t-online.de

Received: 20 February 2024; **Revised**: 7 March 2024; **Accepted**: 15 March 2024; **Published**: 26 March 2024

Abstract: Part of a requisite for natural hazard awareness and damage prevention in Egypt is the detailed monitoring of surface fault zones. The inventory of active faults and their risk assessment is an essential contribution to the safety of settlements, land use and infrastructure (railroads, highways, pipelines) and to damage prevention. Thus, this study aims to contribute to the detection, inventory, and documentation of fault zones. Surface faulting hazard assessment considers any surface consequences caused by surface near faults such as abrupt horizontal and vertical displacements and rotations, or mass movements after stronger earthquakes. Long-term, aseismic, slow-creeping movements along fault zones have to be considered as well. Southern Egypt offers unique and optimal conditions for the research of fault zones and their different structural expressions and conditions because of the dry desert climate conditions and relatively low human influence on the landscape in extended areas, especially for the investigation of different types of faults, their interactions with each other and the outcropping rocks, and fault-related deformation structures. Volcanic activity has been influenced in the geologic past often by larger fault zones as dike intrusions, volcanic cones and plugs or craters occur concentrated along these zones of weakness facilitating the uprise of magma. Larger fault zones are crossing reservoir areas. Surface water intrusions into deep-seated faults have played a role in triggering earthquake swarms in the reservoir areas during the last decades. Mapping of active faults is not only an important but also a cost-intense task when carried out in the field or when using geodetic and geophysical data. In the scope of this study, fault detection was carried out based on different open-source satellite data (Landsat 8 and 9, Sentinel 2 optical data, Sentinel 1 and ALOSPASAR radar data, and Google Earth and Bing Map high-resolution satellite images) from the southern part of Egypt. Faults were digitized using ArcGIS and QGIS software. An inventory of fault-related structural features (depressions, ridges, rotation structures, etc.) and rift zones was elaborated based on remote sensing data. An overview of different types of faults and their related structures as well as their interactions with their host rock conditions could be achieved. By merging the inventory results with infrastructural and land use data, critical areas with potential damage risk were pointed out.

Keywords: fault zones; fault related structures; remote sensing; GIS; southern-Egypt

1. Introduction

An important input to damage mitigation and natural hazard preparedness comprises surface fault assessment. It considers any surface consequences such as abrupt horizontal and vertical displacements, rotations, or secondary effects like mass movements and soil instabilities along fault zones after stronger

earthquakes. A surface rupture can occur suddenly during an earthquake or more slowly over time. Surface ruptures during earthquakes often happen along preexisting faults. Thus, it makes sense to map and consider the existing fault network. Surface rupturing, whether co-seismic or creep-induced, may cause even catastrophic damage, especially when lifelines pass through it [1]. Figure 1 shows an example of roads crossing two active fault zones in the west of the Aswan Reservoir in southern Egypt. Damage of the roads crossing the fault zone segments can be expected in this area not only due to stronger ground motion related to reflections and interference of seismic waves, vertical and/or horizontal displacements, but also due to the slowly ongoing, creeping, long-term movements [2]. The consequences of long-term, aseismic and slow, creeping movements along fault zones are often underestimated, but they can cause considerable damage to the infrastructure as well by accumulating effects over time. Unstable ground conditions along the fault zones because of associated related fault structures such as subsidiary fault systems, ridges, rotation blocks and depressions, might affect the stability of infrastructure as well. For the surveillance and maintenance of the infrastructure such as the road network, precise knowledge about fault zones and their properties is essential. This study aims to contribute to the awareness of this necessary data mining.

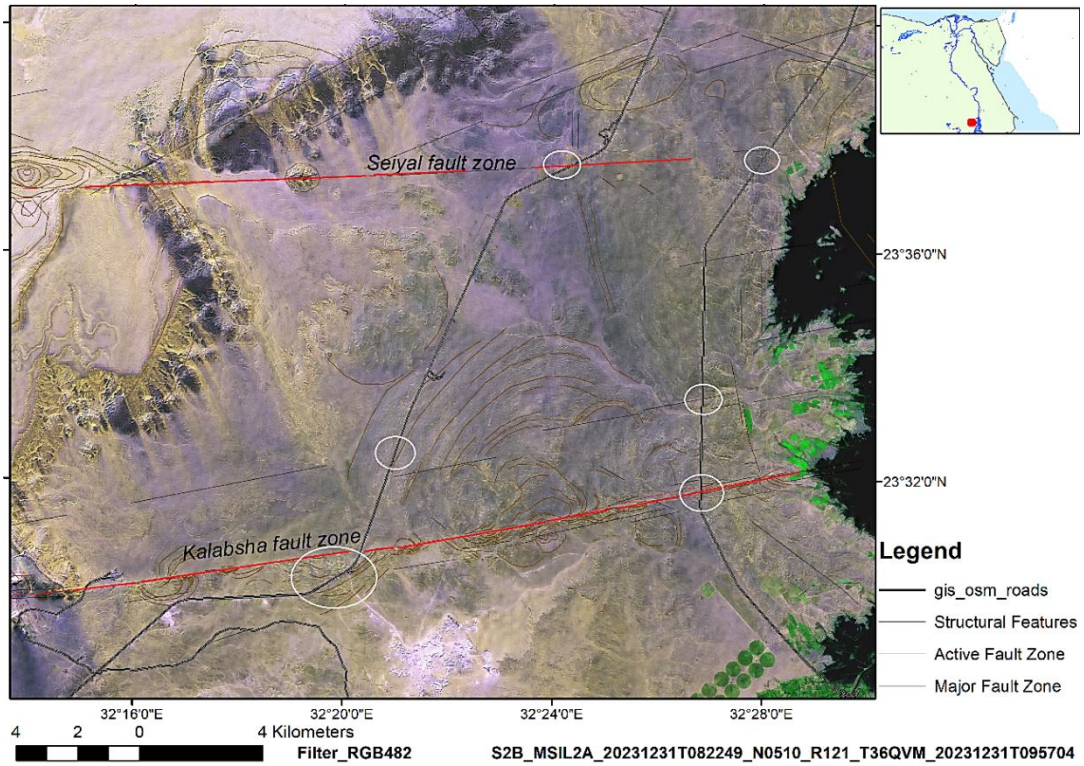

Figure 1. Highways (black lines) and irrigation fields (green), crossing active fault zones (red lines) combined with the evaluations of a Sentinel 2-satellite image. The white circles indicate road segments situated within fault zones and related structures (dark-brown lines). The road-shapefiles were downloaded from [3].

Fault zones are crossing the Aswan Reservoir area as well. The question arises of how these active faults might affect the reservoir areas. Besides the increasing water load because of the dam, the fluctuations in the reservoir water level after rare heavy rains in this area and after flash floods will increase the water weight and, thus, the pore pressures in the rocks. Increased seismicity during the last decades within the reservoir areas has been documented [4,5]. Along the larger fault zones surface water can infiltrate into the subsurface. More fluids in larger depths can trigger earthquakes within already stressed fault planes. Reversed, high permeable zones may play a role as pathways for the up-flow of hydrothermal fluids. Thus, the documentation of faults, their types and properties is a necessary step towards potential damage mitigation with regard to the reservoir area.

Special attention is directed to traces of active fault zones. A fault is considered active if there is evidence of distinctly visible displacements at the surface without or only a few traces of erosion [6]. Evidence for fault activity is typical structural features such as pull-apart basins and depressions or push-up ridges along the fault

zones. These dislocated structures can be used to learn the relative age of the fault activity whenever the age of the outcropping rocks is known. Another criterion is the evidence of displacement during the Holocene and the occurrence of earthquakes along this fault zone as well as movements confirmed by geodetic surveys.

Egypt offers ideal and even unique conditions for the research of faults and their different structural expressions because of the dry desert climate conditions and relatively low human influence on the landscape in extended areas, despite the coverage of large areas with aeolian sediments. These conditions allow the research of different types of faults, their interactions with each other and with the outcropping host rocks, and of fault-related structural features. Although several selected areas in Egypt have been investigated very detailed, some fault zones are still not documented yet for example in geologic maps or the GEM Global Active Faults Database (GEM GAF-DB) [7,8]. Fault systems in Egypt have been mapped in the field, derived from geophysical data, satellite imageries and digital elevation data, but some tectonic features may have been missed so far because of the widespread sedimentary covers or all the difficulties in carrying out fieldwork in remote areas.

This study is focused on the southern part of Egypt, where prominent E-W and N-S striking faults occur that are tens to hundreds of kilometers long such as in the Western Desert of Egypt [9]. Some of these faults are obviously still active today. Volcanic activity has been influenced in the geologic past often by those larger fault zones, building zones of relatively "weakness" and, thus, facilitating magmatic intrusions such as dikes, volcanic plugs and cones, or the development of craters. Stronger earthquakes are documented in this area with fault plane solutions with the same orientation representing major dextral (right-lateral fault movement in which the fault moves to the right from the viewer's point of view) shear movements [10].

2. Materials and Methods

This study deals with the evaluation of optical satellite data as well as of radar images with the radar specific penetration capabilities into dry soils up to several meters and on Digital Elevation Model (DEM) data and DEM-derived morphometric maps aiming to detect traces of fault zones and their related structures. Special attention is directed towards the inventory of different types of fault zones, their kinematics, their hosting outcropping rocks, and their surrounding tectonic setting based on remote sensing data, combined with other geoscientific data of southern Egypt. Of course, the evaluation capabilities of satellite data are limited, and further research is required to clarify the spatial and structural fault details. Therefore, one goal of this study is to provide hints and point out directions where future field research or other surveys could be focused to answer open questions. Mapping active faults is not only an important, but also a difficult and cost-intense task that contributes to the safety of settlements, cities, and infrastructure [1]. Thus, it is a requirement for land use planning. There are several methods to analyze fault zones, among them:

- The study of natural exposures of fault zones in the field helps to detect whether a fault is still active inherited from past ruptures and dynamics, or both due to reactivation. Whenever these faults are covered by younger sediments their detection in the field becomes difficult.
- Geodetic measurements proving movements and providing data about ongoing slip rates are other important tool to detect geodynamic activities along the fault zones. However, this method is cost- and time-intensive, and, thus, the availability of geodetic data in SW and Central S-Egypt is still incomplete[11].
- Geophysical methods are used to determine the often buried faults (aeromagnetic survey, seismic and gravity data analysis, etc.) [12]. Earthquakes along larger fault zones with fault plane solutions indicating similar spatial characteristics (fault geometry: strike, dip, length) as the surface near the fault can indicate active processes. Stress leading to ruptures is either released during earthquakes or by continuous aseismic frictional sliding or aseismic fault creep [13] leading to traces of deformation within the youngest sediments that can be observed on high-resolution satellite images.
- Remote sensing data provide an important input to the overview, inventory and understanding of the kinematic development of fault zones, especially the higher resolution satellite data. These data allow the creation of a quite detailed information base.

The evaluations of different satellite data and available geodetic and geophysical data were carried out as summarized in the next figures (Figures 2 and 3). Sentinel 1 Synthetic Aperture Radar (SAR, C-Band radar wavelength), ALOS PALSAR (L-Band wavelength) radar data and optical Sentinel 2 images, ASTER, and Landsat 8

and 9 (Operational Land Imager-OLI) were digitally processed and evaluated. The Advanced Land Observing Satellite (ALOS), Phased Array type L-band Synthetic Aperture Radar (PALSAR) from the Japan Aerospace Exploration Agency (JAXA) [14] provided data with 12.5 m spatial resolution. The Sentinel 1 and ALOS PALSAR radar missions included dual-polarization capabilities. It can transmit a signal in a horizontal (h) or vertical (v) polarization, and then receive in both h and v polarizations. RGB- tools were used to merge radar images with different polarizations and, thus, get "false-colored" radar images improving the evaluation possibilities, for example by Sentinel 1-vh, vv, vh polarization composites. The different radar wavelengths correlated with the L-Band (23.5 cm) and C-Band (5.6 cm) allow varying penetration depths into the surface. L-Band radar signals can penetrate more than 1 m into loose, dry sand sheets. Therefore, evaluations of ALOS PALSAR data are especially valuable for the detection of faults in the desert environment of Egypt. The illumination geometry of the radar signals plays an important role in the visibility of the linear and structural features. Those oriented perpendicular to the radar illumination angle appear enhanced, whereas those parallel to the radar illumination are more suppressed, of course, depending on the terrain morphology. Rough surfaces return large amounts of the transmitted energy to the radar satellite sensors (visible in light gray tones), while smooth surfaces scatter the energy and, thus, have low radar returns such as the water surfaces (appearing black on the radar images). Other factors such as dielectric properties and radar characteristics (frequency, depression angle, polarization) also affect the radar return [15]. The processing of the radar data was carried out using the SNAP software of ESA and the image processing tools integrated into ArcGIS. Digital image processing of the different satellite data and image enhancement methods are used to gain additional knowledge about the structural pattern by combining the satellite-specific evaluations.

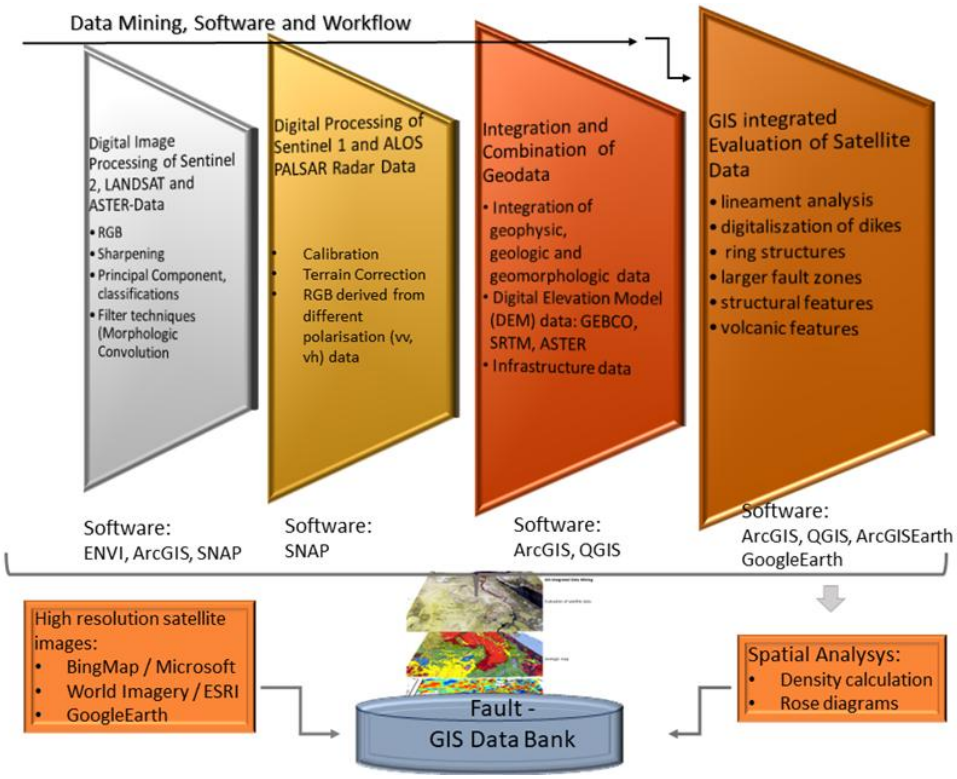

Figure 2. Data sets, software and workflow.

The data were provided by the USGS Earth Explorer [16,17], ESA Copernicus Open Access Hub [18], and NASA Earth Data, Alaska Satellite Facility (ASF) [14]. ALOS PALSAR mosaics were retrieved from the Earth Observation Research Center, PALSAR global mosaic and Forest/Non-forest Map, JAXA [18,19]. Sentinel 2 mosaics were downloaded from the Arab Nubia Group Blog [20] and included in the data sets. The high-resolution Bing Map satellite images from Microsoft and Google Earth images as well as the data from ArcGIS Earth from ESRI were used for detailed mapping.

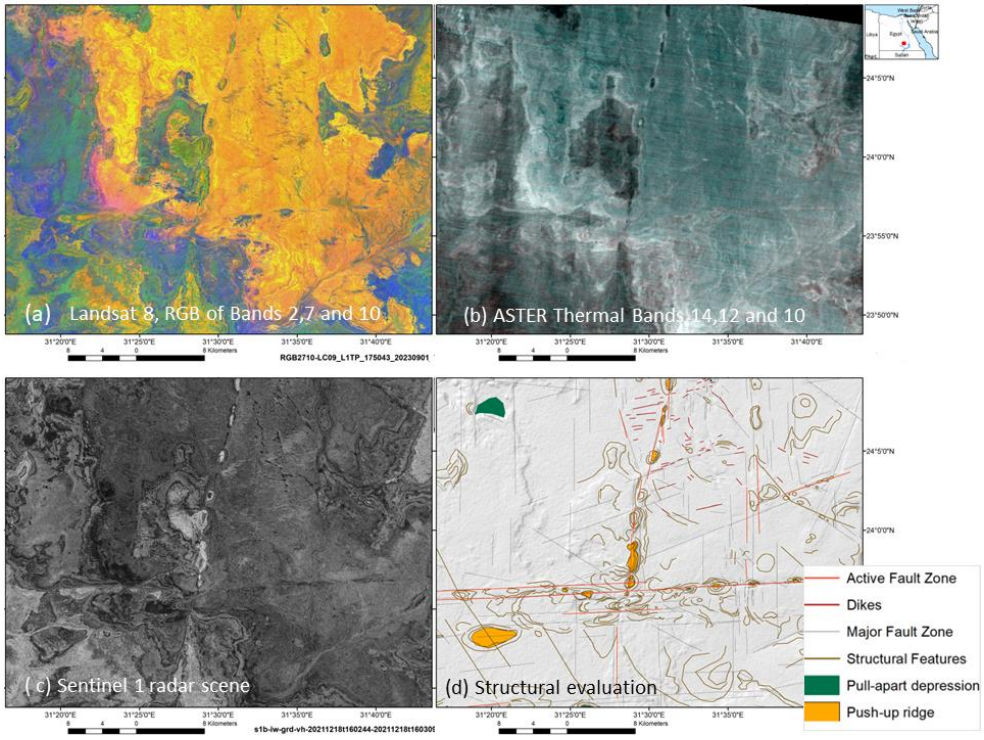

Figure 3. Comparative structural-geologic analysis of different satellite images. (**a**) Landsat; (**b**) ASTER; (**c**) Sentinel 1 radar; (**d**) evaluation.

Digital image processing software served the Sentinel Application Platform (SNAP)/ESA and ENVI/L3Harris Geospatial Solutions as well as Shapefiles were created in ArcGIS related to faults and structural features. For example: Major lineaments, dikes, craters (the term crater is used here as a neutral term just describing the morphology) and circular and oval-shaped structural units were digitized visually based on the different satellite data. Linear features on the satellite images were identified and mapped as faults whenever dislocations of lithologic units were detected or fault-related structures. Especially Sentinel 1 and ALOS PALSAR radar images reveal larger fault zones very clearly. Faults in southern Egypt are often well exposed due to fault scarps and dike intrusions. Dikes that intrude into fault systems support the detection of zones of weakness. These scarps and the dike ridges can be digitized in a GIS as line-shapefiles based on satellite images. The linear traces of faults were merged in a GIS with available geological and geophysical information (geological and geophysical maps [20] georeferenced into ArcGIS and QGIS, earthquake epicenters). Focus was directed toward the inventory of active faults showing distinct traces of deformation like so-called flower structures, pull-apart depressions, sag ponds, or push-up-ridges, indicating horizontal and vertical movements. An example of such an active fault zone with lens-shaped ridges and depressions is shown in Figure 4, and typical flower structures in Figure 5.

Most of the larger faults are assumed to be still active or partly reactivated due to the geodynamic, plate-tectonic situation, and seismic activity. Along the active fault zones, mass movements are observed that have to be considered as a further risk. Take-off areas and mass movements were digitized as far as they were visible on satellite images (Figure 6).

3. Geographic and Geologic Overview

The investigation area comprises a variety of landforms including from E to W the Red Hills, the Nile Valley, the Sinn El-Kaddab limestone plateau [21], the Western Desert, the Nubian Plain, depressions with oases, large dune fields, playas, isolated hills, narrow ridges caused by dikes and the volcanic areas in the SW of Egypt with craters, plugs, scoria cones and lava fields. The widespread Quaternary deposits are represented by different formations such as aeolian sand sheets and dunes, and fluvial sediments accumulated after now rare heavy rains. Traces of magmatic activity form important parts of the landscape as well as traces of tectonic movements. Figure 7 provides an overview of the topography in the study area.

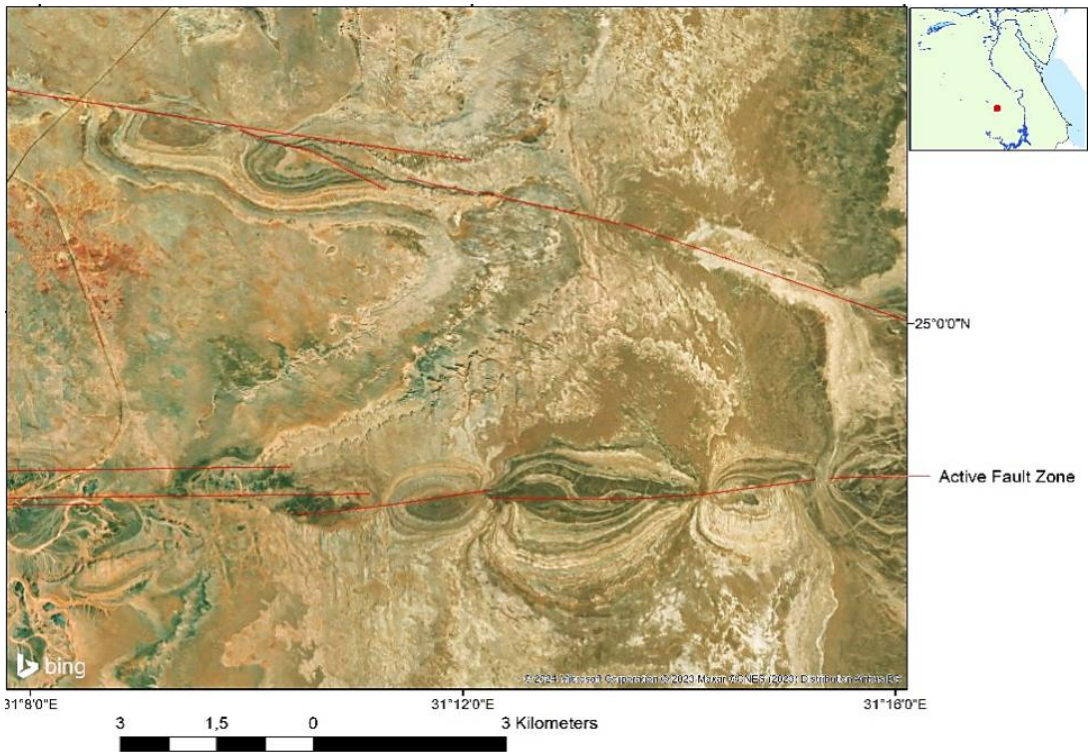

Figure 4. Example of active fault zones (red lines) with visible traces of deformation even in youngest sediments on a Bing Map-scene. Sets of fault-bound rock lenses are bounded by parallel segments of the main fault. Along the strike-slip zone, alternating pull-apart structures and push-up ridges have been formed.

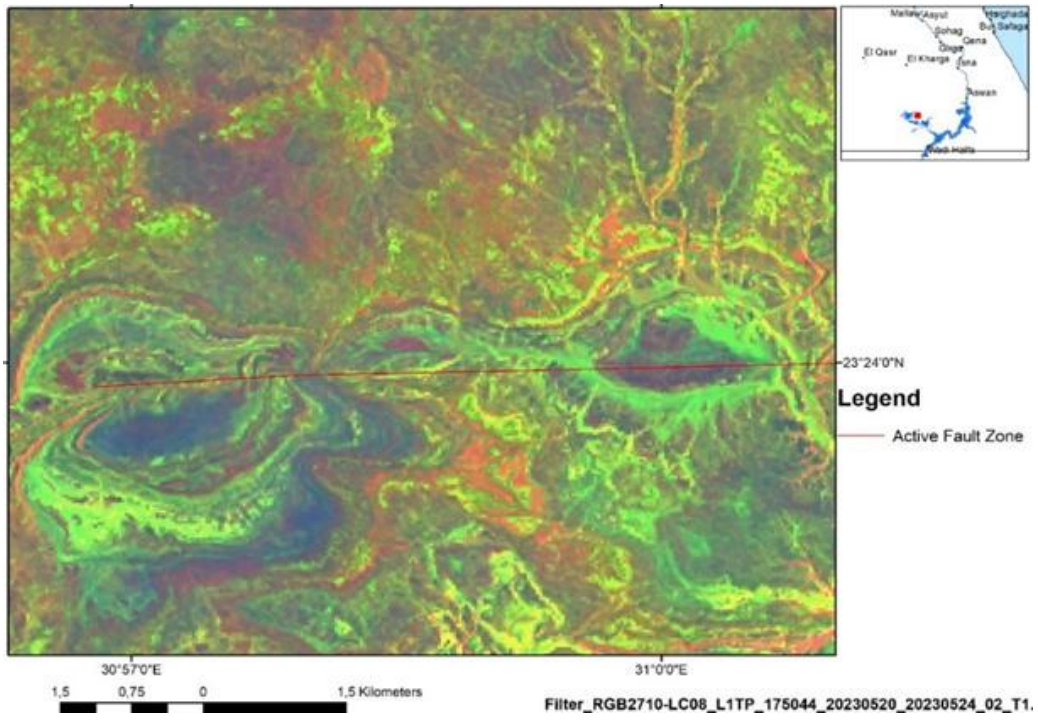

Figure 5. Digitizing a fault with distinct deformation patterns like flower structures and lens-shaped ridges is considered to be still active in S-Egypt, based on Landsat 8-data (RGB combining the bands 2,7 and 10, 30 m spatial resolution).

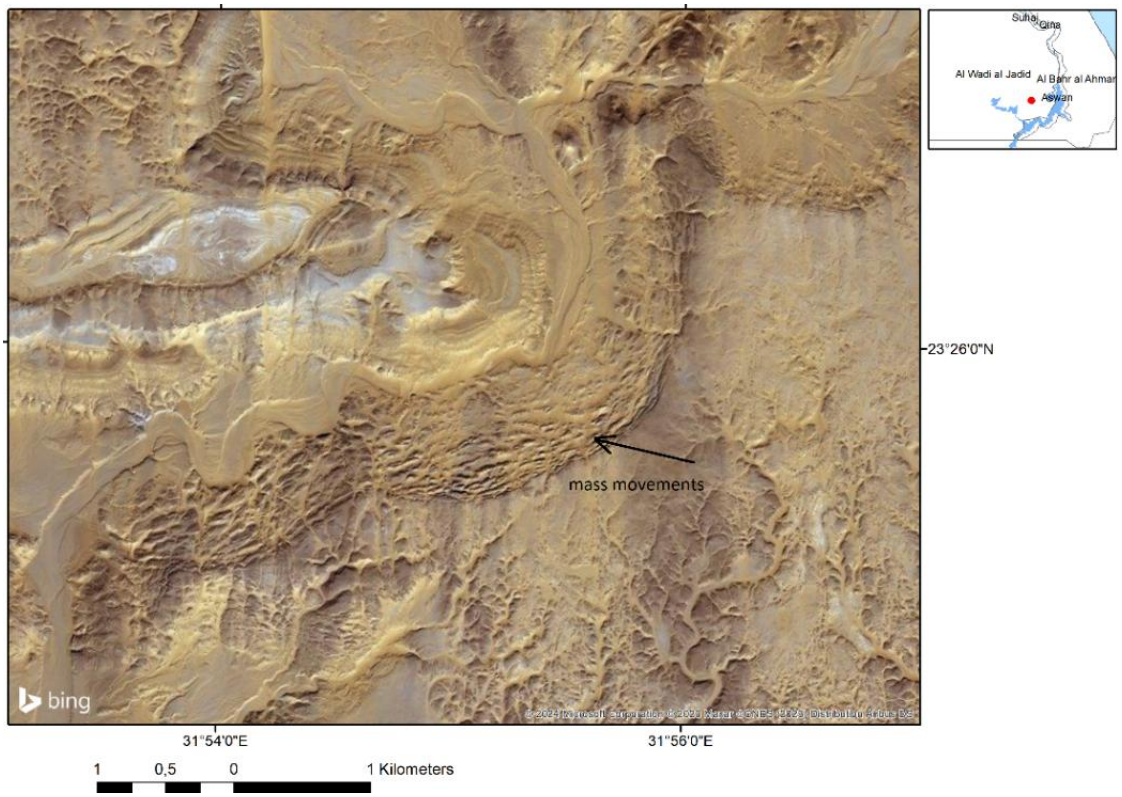

Figure 6. Paleo-landslides or/and still ongoing mass movements (block gliding and rockfall) are visible on a BingMap scene (<10 m resolution).

The present-day stress field is of great importance for understanding the average directions of the maximum horizontal stresses in Egypt and, thus for the development of faults. Stress is either released during earthquakes or by continuous aseismic frictional sliding or aseismic fault creep.

The African Eurasian plate boundary, the Red Sea plate margin and the Levant transform fault represent Egypt's tectonic boundaries [1]. The tectonic deformation in the study area mainly resulted from the interaction between the European and African plates which started in the Pre-Cambrian time and rejuvenated during the Hercynian (Pre-Carboniferous), Laramide (Late-Cretaceous) and Alpine (Late-Tertiary) orogeneses. The basement was affected by two episodes of geodynamic activity and resulting faults; an older one with E-W and N-W axes intersected by a younger N-E set of folds [22].

Due to the intense tectonic compressions from southeast to northwest and from east to west during the geologic past and recent geodynamic activity, fault structures control the tectonic framework of the study area, which is characterized by the superposition of the E-W- and N-S-trending compressive structures. On the Nile Delta, the maximum horizontal stress pattern shows scattered orientations, while on the Aswan region, it has a WNW-ESE strike with pure strike-slip features [11]. The strike-slip movements are associated with an assemblage of related structures, including normal and/or reverse faults. Parts of the study area are located within the Nubian Swell zone, which had undergone tectonic uplift during the Cenozoic, a process that is still episodically active.

The Nubian Fault System (NFS) is extended from the Nile valley across the Western Desert. The NFS is composed of several E-W Principal Deformation Zones (PDZ) characterized by Late Cretaceous to present intra-plate strike-slip faults and related fold structures, as well as regional basement uplifts [23]. The earthquakes in the south of the Western Desert tectonic zone are predominantly related to these strike-slip faults. The deformation style of the NFS is the surface representation of deep shear zones created through the accretion of the Arabian-African shield [23]. Among the NFS in the southeast of the Western Desert, there are three main types: NW normal faults, E-W, ENE and WNW conjugate right-lateral strike-slip faults, and N-S, NNE and NNW conjugate left lateral strike-slip faults [23].

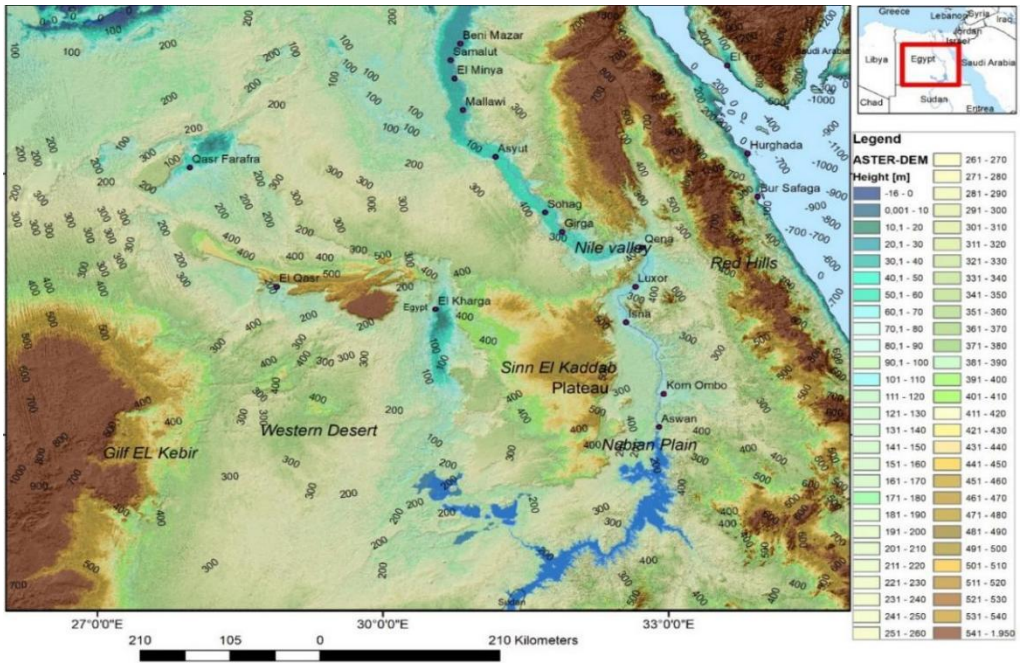

Figure 7. Height level map of central and southern Egypt based on ASTER DEM data.

Mapping and understanding of the relationships between geometric elements of fault systems such as overlap zones, drag, block rotation and variations in fault throw are essential not only for general geological knowledge, but also for land use planning, agriculture (sprinkler irrigation), civil engineering and maintenance of infrastructure.

4. Results

On satellite images, the active faults are often revealed by fault scarps and dislocations as well as by the associated structures or dike intrusions. Figure 8 provides an overview of the mapped faults based on remote sensing data and based on geologic maps. The different segments of the master faults and subsidiary faults are recognizable in those areas with outcropping rocks not covered by aeolian and fluvial sediments.

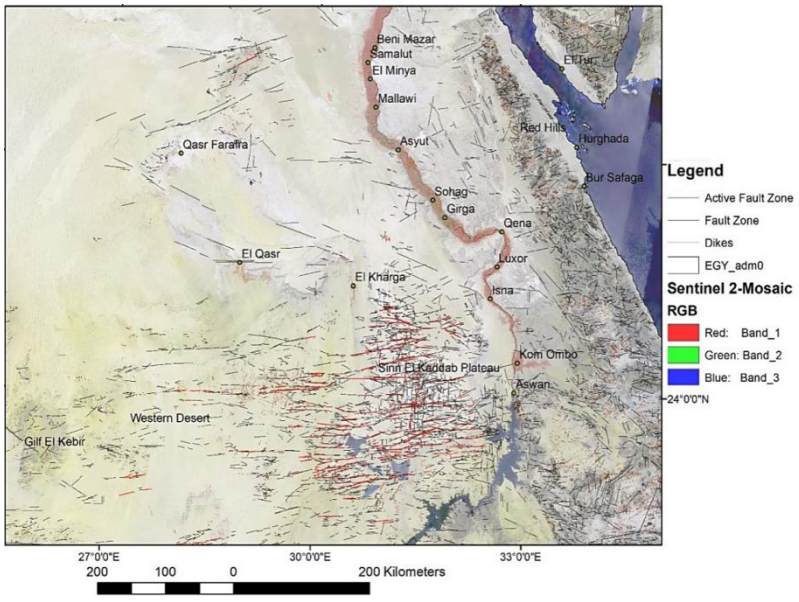

Figure 8. Overview of the main faults in southern Egypt derived from evaluations of satellite data. The Sentinel 2 mosaic in the background was downloaded from the Arab Nubia Group Blog [19].

An overview of the fault pattern and the different types of fault zones in southern Egypt as derived from satellite images is shown in Figures 9a,b:

- Faults in volcanic areas in the Gilf El Kebir area in the SW,
- fault systems in areas with sedimentary strata, mostly Jurassic sandstones in the Western Desert, belonging to the Nubian fault system,
- faults in the Eocene and Paleocene limestones and shales of the Sinn El Kaddab Plateau,
- faults in the metamorphic and igneous Precambrian basement (granitic and gneissic rocks), of the Red Hills in the southeast. The faults in the Red Hills generally rarely show traces of fault-related structures on satellite images, however, a lot of dike swarms along zones of less resistance to intrusions.

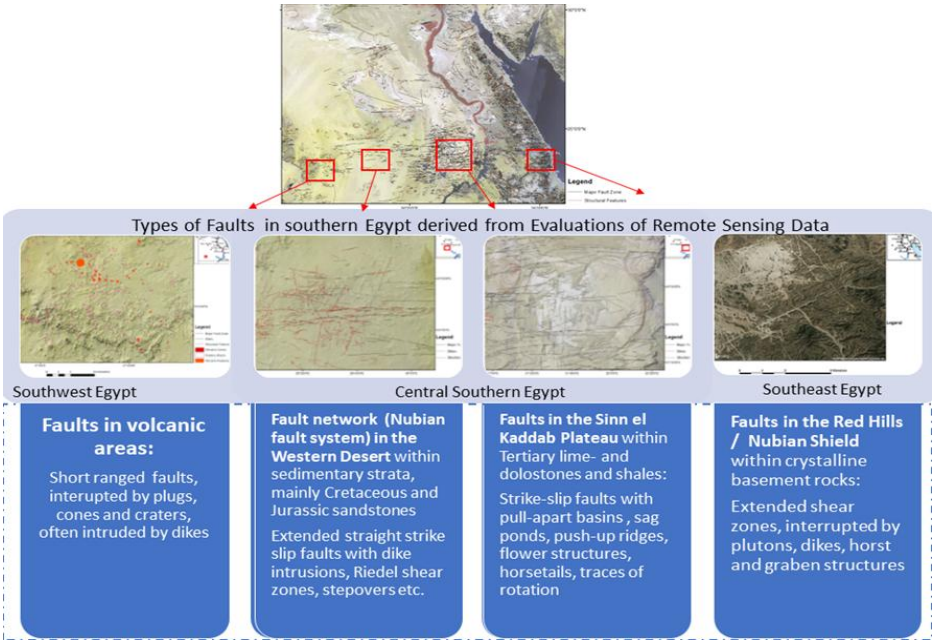

(a) Fault patterns and types of faults derived from the evaluations of remote sensing data.

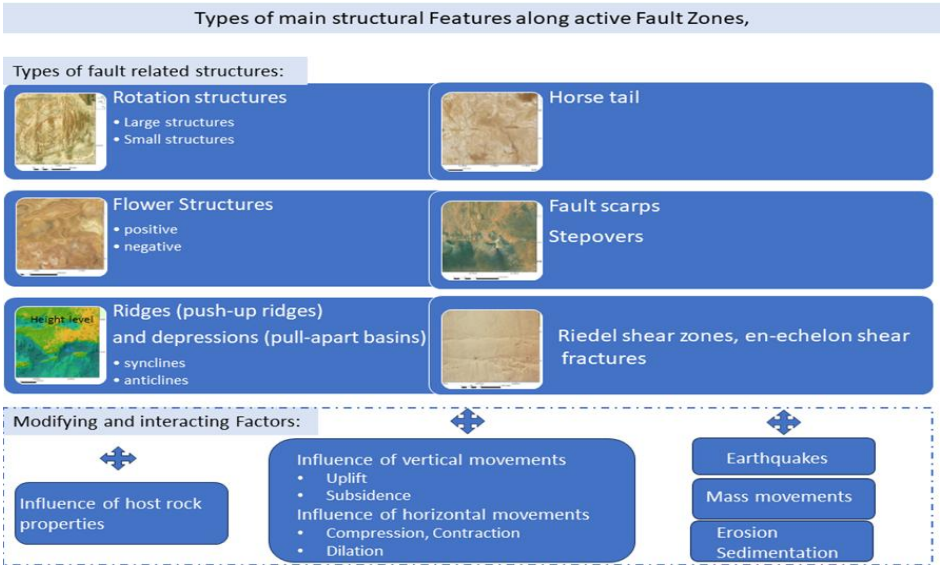

(b) Overview of various types of fault related structures and modifying factors.

Figure 9. Overview of the main fault types and fault related structures.

The mapping of fault zones as shapefiles in ArcGIS allows density calculations of faults with related structures considered to be still active or potentially reactivated (Figure 10). The highest density is observed in the Sinn El Kaddab plateau and the Western Desert. Therefore, these two areas will be investigated in more detail. Flower structures, pull-apart depressions and push-up ridges, as well as rotation structures, were digitized, and their spatial occurrence was analyzed.

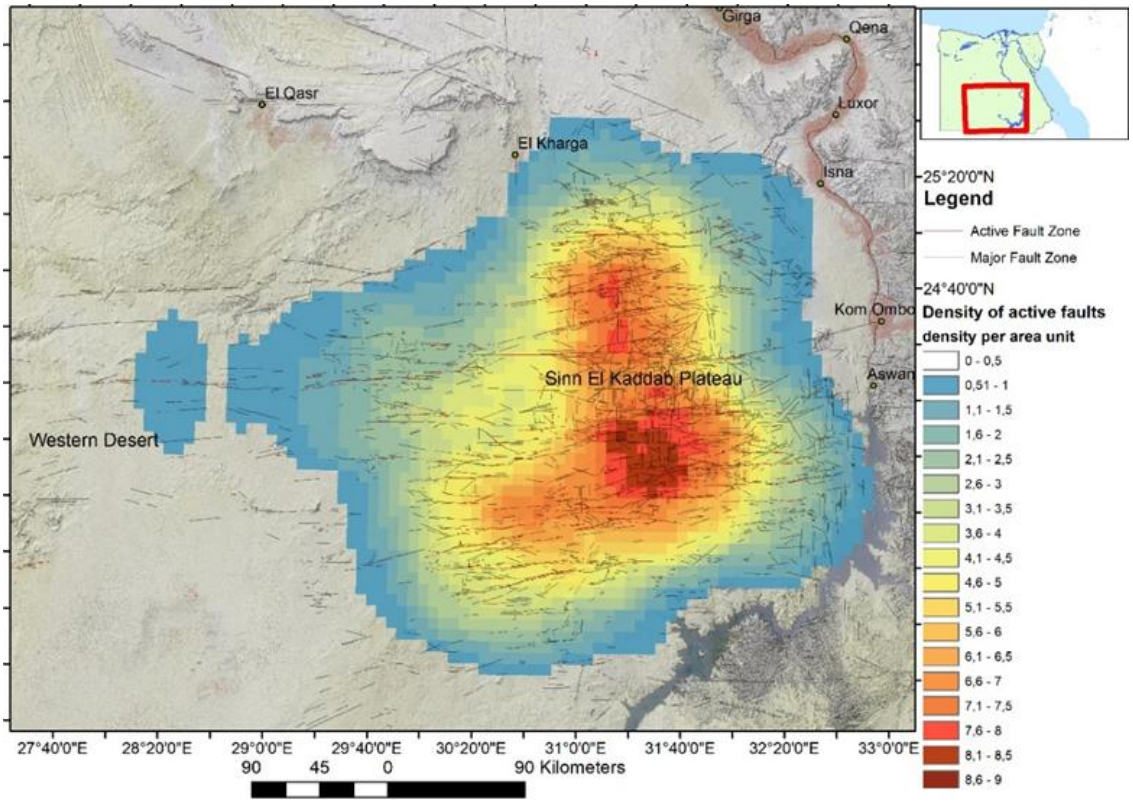

Figure 10. The density of active fault zones mapped based on satellite images calculated in ArcGIS in the central part of southern Egypt.

4.1. Fault Mapping Based on Evaluations of Satellite Data of the Sinn El Kaddab Plateau and Overview of Fault Related Structures

The height level of the Sinn el Kaddab Plateau varies from 220 to 550 m above sea level. The plateau is a flat tableland comprised of Late Cretaceous to Early Eocene limestones, marls, shales and sandstones, dissected by numerous east-west trending, strike-slip faults along which related depressions and ridges formed due to relative movement along these faults [9]. Ductile and brittle deformation styles are observed along the deep-seated, E-W and N-S trending active fault systems [21]. The slip rates on E-W faults are estimated to be about 0.03 mm/year. N-S faults have lower slip rates, about 0.01 to 0.02 mm/year [10]. These movements are still active and ongoing due to plate tectonic dynamics. The recent geodetic data and GPS measurements imply that the African plate is moving NW with respect to Eurasia with a velocity of 6 mm/year and the spreading rates along the Red Sea decrease from 14 mm/year at 15° N to 5.6 mm/year at 27° N [24,25].

Regional stress patterns can vary and rotate significantly within major tectonic fault zones, especially in areas of intersecting faults or changing host rock properties. The mechanisms responsible for such stress changes and rotations are complex, depending on the fault structure, fault zone rock mass rheology, and in situ pore pressure [26]. The kinematics and mechanics of strike-slip faulting are well displayed on the different satellite images of the area [27]. However, the evaluations of the different satellite images show as well as the complexity and interactions of the fault pattern, especially when intersecting each other. Figure 11a provides an overview of the structures related to the active faults of the Sinn El Kaddab and adjacent areas and Figure 11b provides an amplified scene from the SE border of the Sinn El Kaddab Plateau showing the Seiyal and Kalabsha

faults.

The structural geomorphic landforms are the result of basement rock uplift of the area accompanied by extensional fault propagation. The area had been affected by tectonic uplift since the Cenozoic, a process which is still considered to be episodically active [21]. The regional basement uplift has played a noteworthy role in the structural pattern of the area [10].

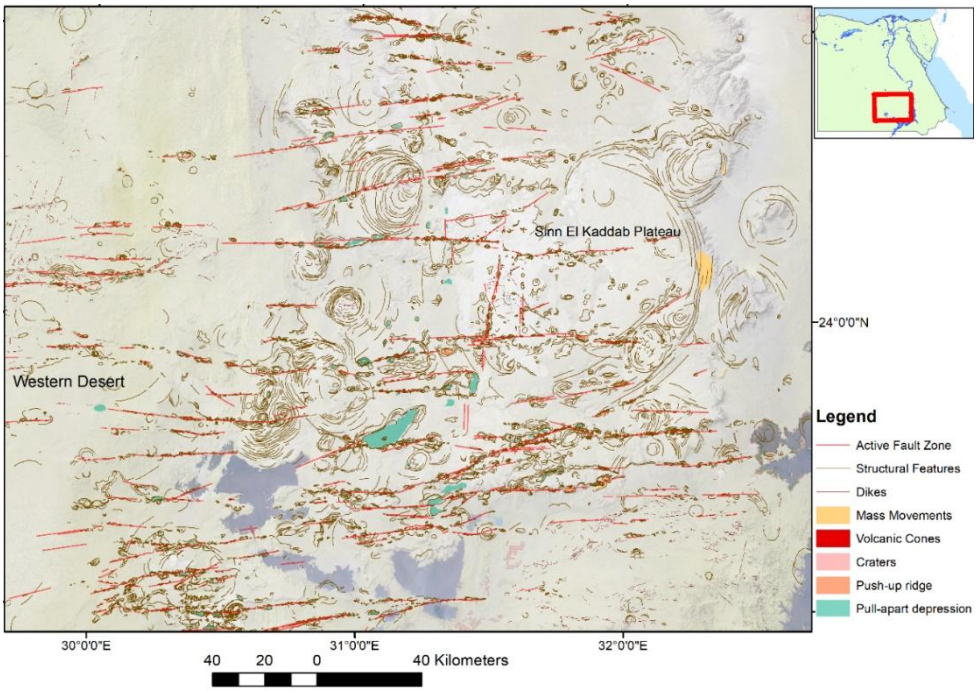

(a)

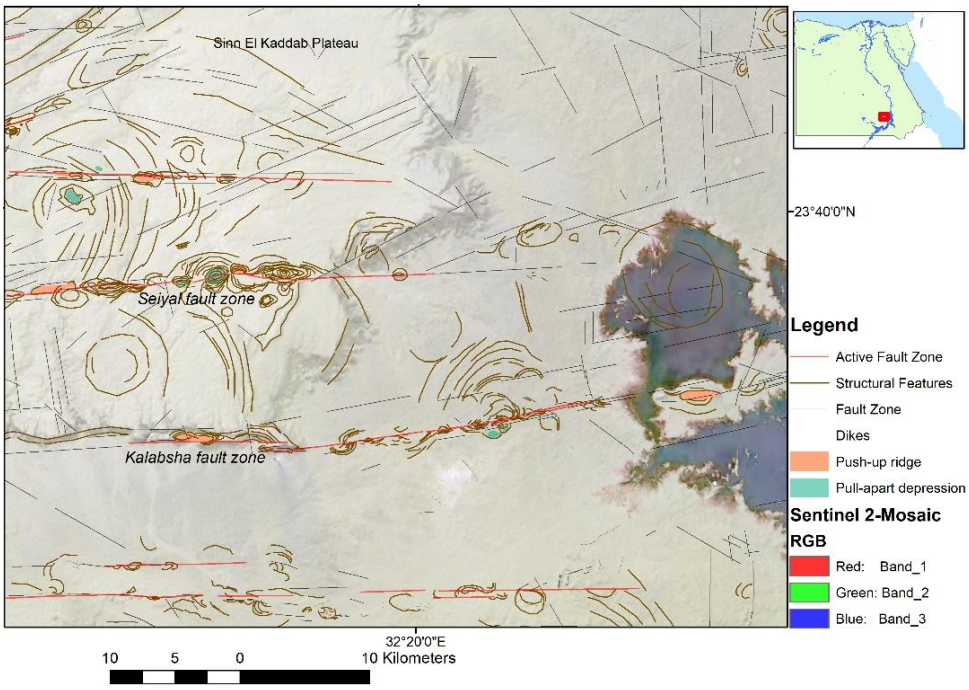

(b)

Figure 11. Structural evaluation. (**a**) Digitized traces of fault zones (red lines indicate faults with associated pull-apart depressions und push-up ridges) in the Sinn el Kaddab Plateau and adjacent areas and of traces of circular features; (**b**) amplification of (a) from the southeastern border of the Sinn El Kaddab Plateau.

The Western Desert and the Aswan area in South Egypt are prone to continuous seismic activity because of seismogenic active faults, particularly the Kalabsha and Seiyal active E-W faults. The Kalabsha fault is approximately 300 km long and is one of the most active faults in the study area. A strike-slip motion with an extension component of 0.6 mm/year is estimated by [25]. Along the major fault zones like the Kalabsha fault along the southern border of the Sinn el Kaddab Plateau slope failure such as block gliding can be observed. The east-west oriented Seiyal fault is approximately 100 km long [9]. It is not a single fault, it is a segmented fault zone including step-overs and bends, partly reactivated along the different segments. During the deformation, significant differences in the deforming process are possible between fault segments because of differences in the mineralogic compositions, mechanical properties and stress distribution.

The next Figure 12 shows earthquake epicenters along the larger fault zones indicating geodynamic movements. The epicenter of the magnitude 5.6 earthquake that shook the area southwest of the Aswan High Dam in 1981 occurred along the Kalabsha fault system. The earthquake data were provided by [28-30].

Most of the seismicity data recorded in the study area are concentrated at the intersection of the North-South (Kurkur and Khor El-Ramla faults) and East-West (Kalabsha and Sayal) faults with the Nasser Lake [1,2], as shown in Figure 12. The seismicity around the lake is characterized by a strike-slip pattern. The High Dam's region is affected by N-S faults, which appear to be vertical and extend reaching the granitic basement [12]. These faults are the Spillway Fault, Powerhouse Fault, and Channel Fault of the River Nile itself [31]. These fault planes have been probably repeatedly active with a polycyclic motion history, including normal growth phases, reverse growth phases and inactivity phases. This leads to complex and repeated reactivation of faults and fault segments resulting in a complex structure and stratigraphy.

Faults can be dormant for considerable periods. Even when not active anymore these zones of weakness could be reactivated during stronger earthquakes or prone to earthquake-related secondary effects like slope failure or subsidence. Propagating earthquake shock waves can induce dynamic fracturing and fragmentation that effectively change the mechanical properties of fault zone rocks and, thus, influence local site conditions during stronger earthquakes. These complex interactions should be taken into consideration when dealing with hazard awareness.

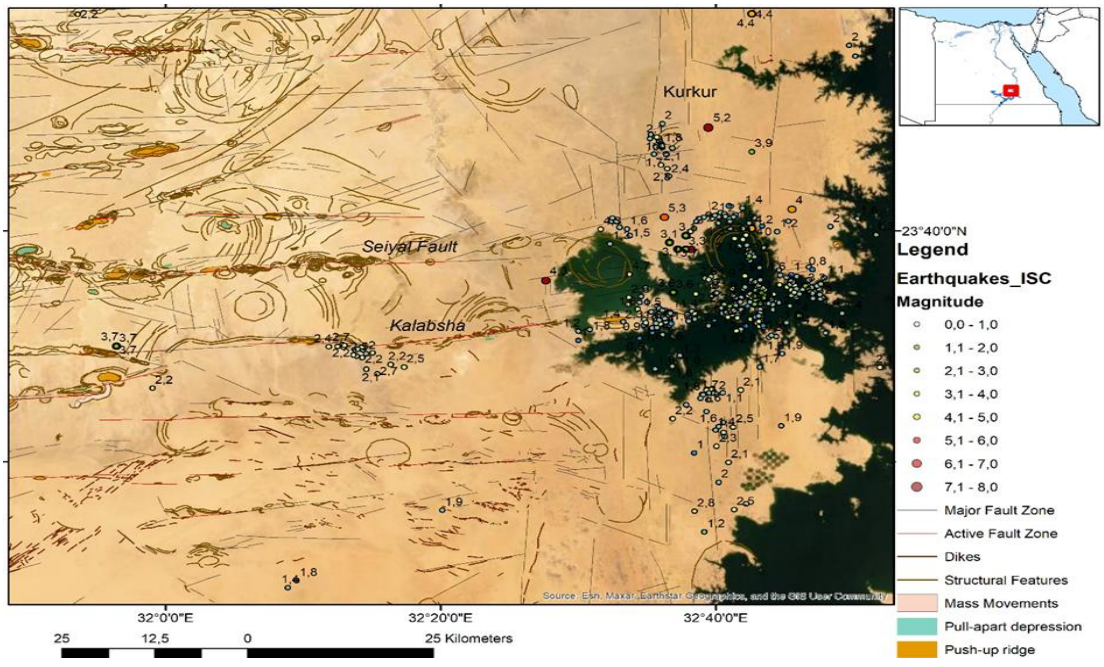

Figure 12. Earthquake epicenters [28–31] in the area of the southern Sinn el Kaddab-Plateau and reservoir area and fault zones visible at the surface. Along the Kalabsha fault, a strike-slip motion with an extension component of 0.6 mm/year is estimated [25]. Lens-shaped pull-apart depressions, sag ponds and push-up ridges can be observed in the satellite images.

4.1.1. Pull-Apart Depressions/Basins and Push-Up Ridges

Strike-slip movements can be associated with an assemblage of second-order related structures [32]. Pull-apart basins and lens-shaped depressions can develop at releasing steps during fault interaction [33]. However, when analyzing depressions in areas with outcropping limestones it is sometimes difficult to differentiate between sinkholes and depressions created by kart processes and sag ponds or pull-apart basins due to strike-slip movements, especially in case of intersecting fault zones. Karst landforms are widespread all over the plateau region due to the presence of the Eocene carbonate rocks [34].

Strike-slip rock lenses may be of compressional or extensional origin, depending on whether they formed at an extensional (facing towards the movement direction) or contractional (facing against the relative movement) bend [33]. In large systems, pieces from one side of the main fault may be sliced off and transferred to the other side as the active fault takes a new course. This may produce far-traveled blocks that are exotic to the block with which they are associated. Blocks of this type have been transported to a considerable distance from their sites of origin.

In general, it was assumed if a major strike-slip fault produces a pull-apart depression or basin, the trace of a fault should not run through the middle of the pull-apart basin [35]. It will mostly likely run through the margins of the basin and always away from its center. However, when evaluating the satellite images of southern Egypt, it seems that during the ongoing neotectonic activity traces of displacements could be found cross-cutting directly through the fault-related structures (see also Figure 5). They are aligned along the main fault. As the satellite images cannot provide height information, digital elevation model (DEM) data were included in the investigations. SRTM DEM and ASTER DEM data with about 30 m and ALOS PALSAR height data with 12.5 m spatial resolution indicate smaller depressions along the larger fault zones (Figure 13). Thus, it was possible to verify depressions and ridges and digitize them as polygon-shapefiles. The detection of pull-apart depressions and push-up ridges is supported by the combined analysis of high-resolution satellite images such as those provided by Bing Map/ Microsoft with the digital elevation data.

In areas with outcropping limestones, it is sometimes difficult to distinguish along larger fault zones between sag-ponds and karst sinkholes or depressions affected by both, tectonic and karstification processes.

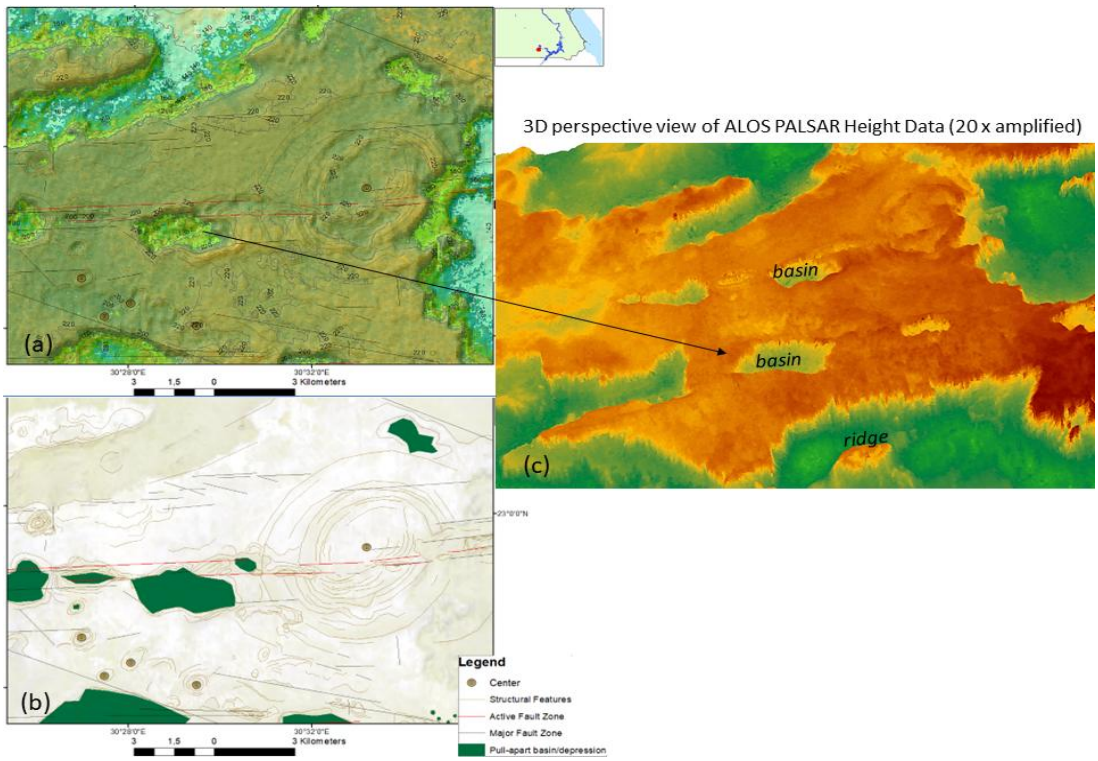

Figure 13. Use of DEM data to identify basins and depressions. (**a**) Height level map; (**b**) evaluation; (**c**) 3D perspective view of a height level map based on ALOS PALSAR DEM data.

Due to the subtle radar backscatter depressions and ridges become visible on Sentinel 1 and ALOS PALSAR radar images (Figure 14a). Figure 14b shows examples of pull-apart depressions and push-up ridges along fault zones within the Sinn el Kaddab-Plateau. Most of the oval-shaped, elongated depressions can be detected on radar images in dark gray or black tones because of the mirror-like radar reflection of flat, sand-filled basins. An example of a rhomboid pull-apart basin is presented in Figures 14a,b. Creating a RGB image by using Sentinel 1 vertical-horizontal polarization (vh), vertical-vertical polarization (vv) and again the vh-images, a color-coding of the radar image was achieved (Figure 14b).

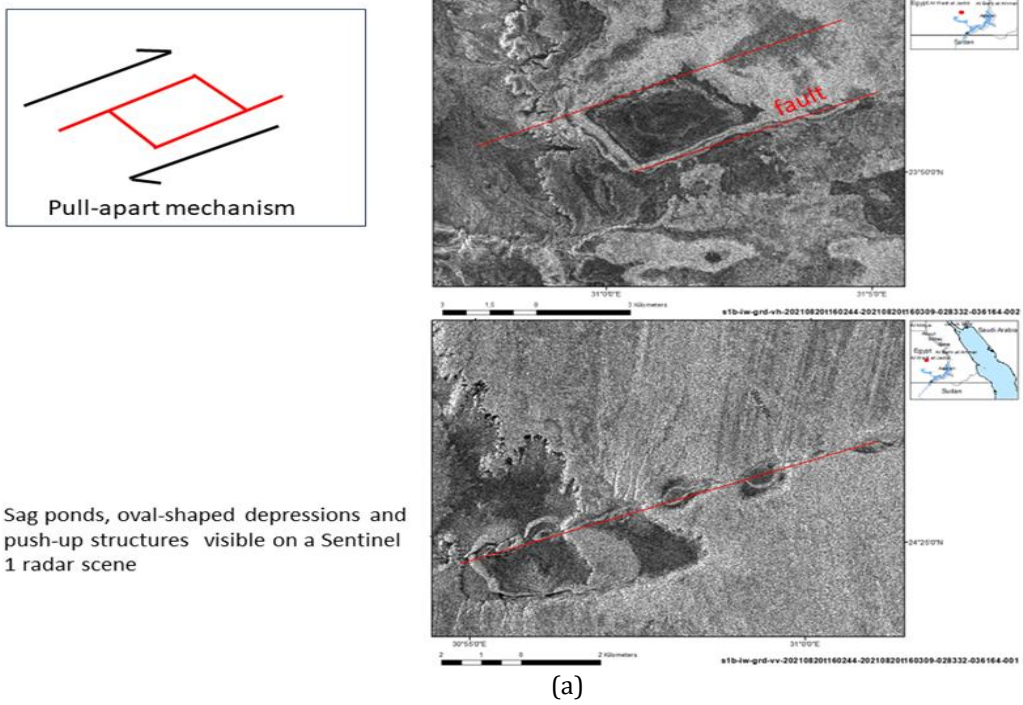

(a)

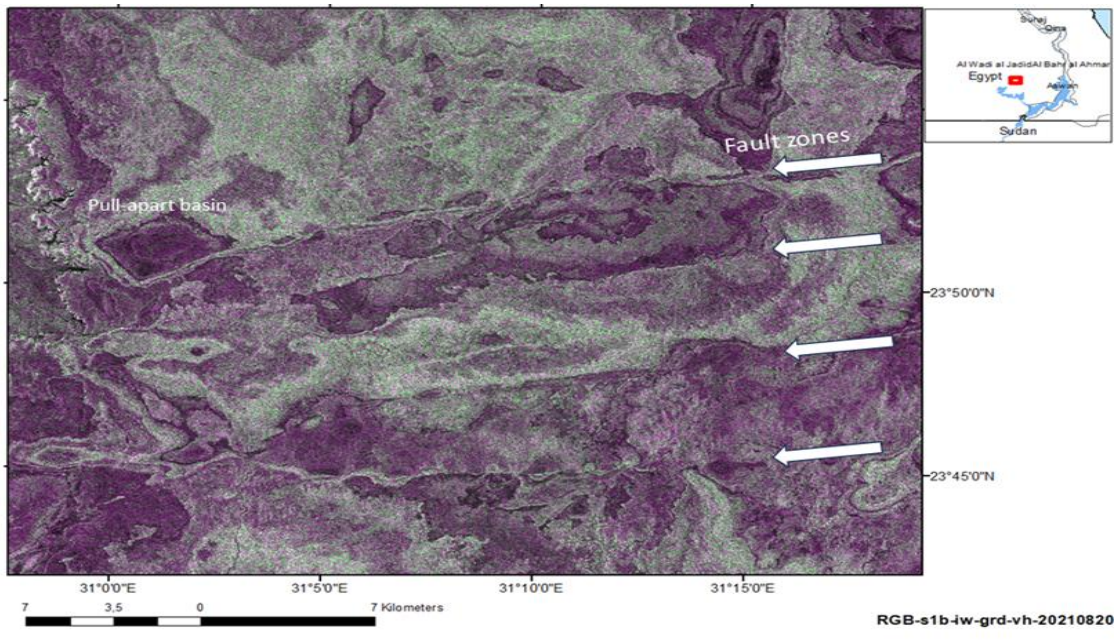

(b)

Figure 14. Detection of pull-apart basins and fault zones on radar images. (**a**) Small-scale pull-apart structures visible on Sentinel 1 radar RGB scenes; (**b**) Shear zones leading to the development of pull-apart depressions.

Figure 15 provides a diagram of the depression lengths, whereby the larger ones occur concentrated in the western and southern part and the southwestern adjacent areas of the Sinn el Kaddab Plateau, and Figure 16 provides a diagram of the length of the ridges. Most of the lens-shaped depressions along active fault zones show lengths of about 100 m up to kilometers. The ridges vary in their size more than the depression, depending on the lithologic properties of the host rocks.

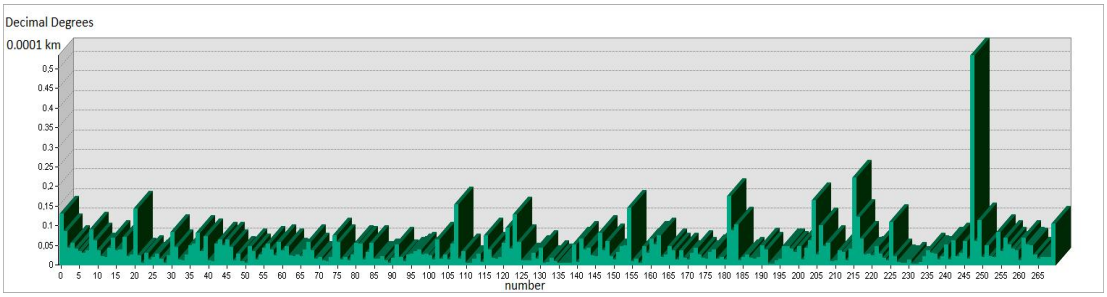

Figure 15. Length of depressions.

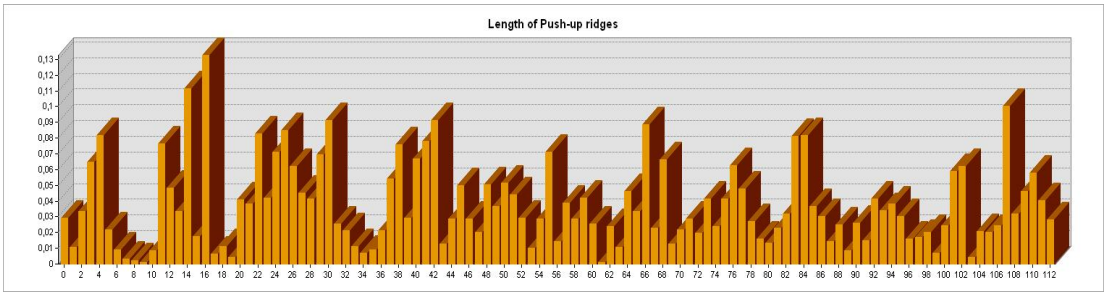

Figure 16. Length of ridges.

Density calculation of fault-related structures in ArcGIS-implemented tools supports the detection of stress field patterns implying that the higher concentration for example of sag ponds or depressions corresponds to higher stress levels. When calculating the density of depressions and pull-apart basins, their concentration in the western and southwestern part and border of the Sinn el Kaddab-Plateau becomes obvious (Figure 17). Most of the pull-apart basins and oval-shaped depressions occur in its western part and along the western border.

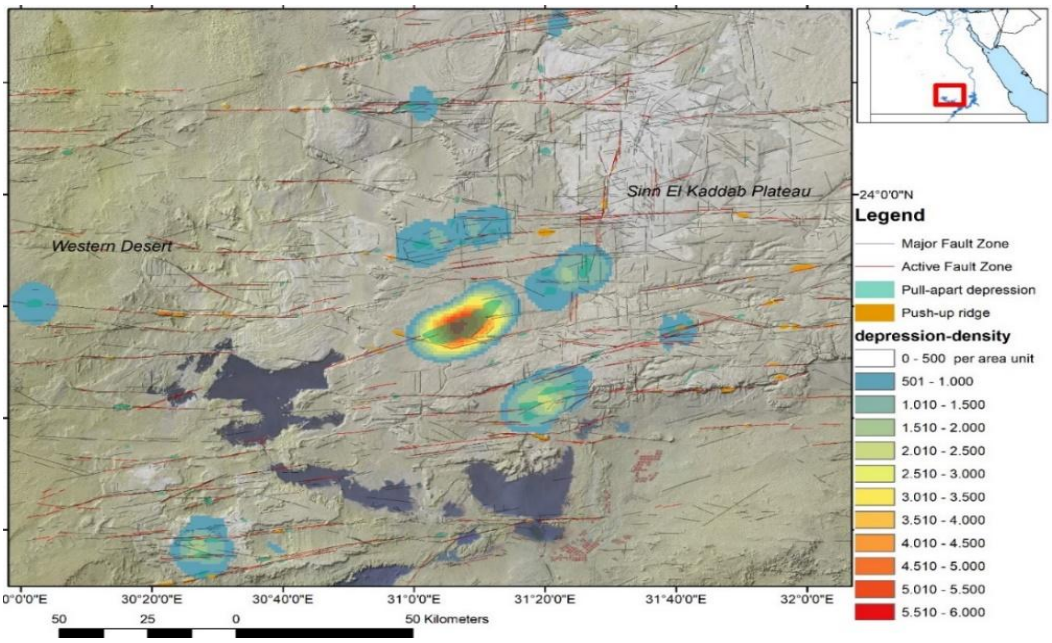

Figure 17. Density of pull-apart basins and oval-shaped depressions along larger fault zones.

4.1.2. Flower Structures

Within the Tertiary rocks of the Sinn el Kaddab Plateau, rocks are deformed as so-called flower structures along strike-slip faults. The term "flower structure" reflects the resemblance of the structure to the petals of a flower. Flower structures frequently appear between parallel fault segments. In plan view, flower structures are mainly located where faults are bounded by subparallel principal faults, or between an array of non-connected subparallel faults [36]. The geomechanical properties of the lithologic units play an important role during the deformation process: After the initial period of elastic deformation, a critical point of elastic deformability is reached. In this case, the material, instead of fracturing, is assumed to accommodate itself to the applied forces by rearranging its internal structure. The result is plastic deformation, which will continue as long as the forces are applied.

Figure 18 shows an example of flower structures visible on different satellite images. Each type of satellite image provides specific information about the surface, for example, the radar images about the radar backscatter characteristics depending on the surface structure and texture, and the Landsat RGB combination including 2 thermal bands about the surface brightness properties. Thermal inertia controlling surface temperatures supports the identification of faults and their related structures. High-resolution images of World Imagery files and ArcGIS Earth/ESRI and Bing Maps Aerial/Microsoft allow the detection of more details due to their higher spatial resolution.

It cannot be derived from remote sensing data, whether the vertical movements of the flower structures are positive or negative. In the case of the area presented in Figure 18, the part of the flower structures south of the main fault is well developed whereas in the north the affected area is smaller covering just the northern border of the flower structure.

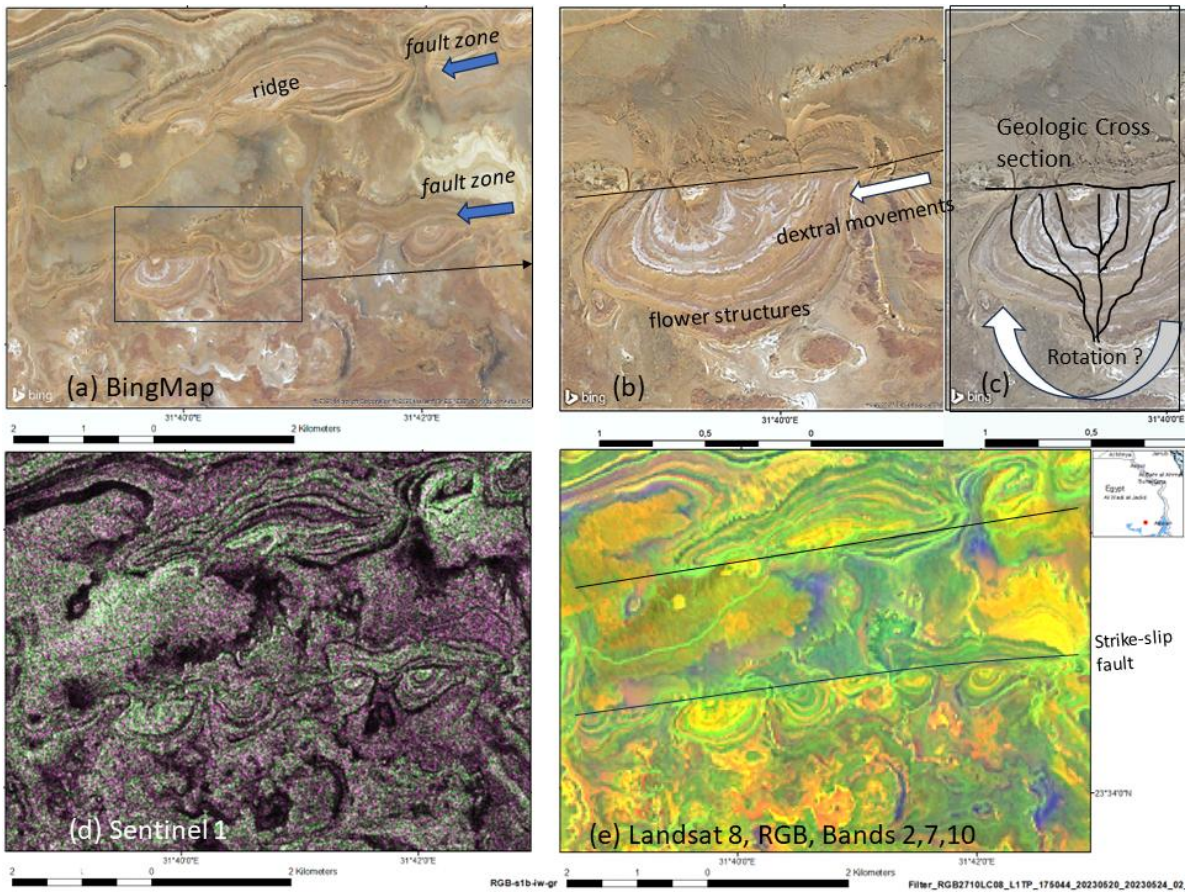

Figure 18. Flower structures as a result of a plastic deformation. (**a**) BingMap scenes; (**b**) BingMap scenes; (**c**) a schematic geologic cross section; (**d**) Sentinel 1 radar scene; (**e**) Landsat 8 scene.

When analyzing the fault zones embedded in shales and limestones and their structural expressions it can

be assumed that their development might have been influenced during more humid climate conditions in the past, allowing a higher ductility along the fault zones within marls and shales. Slope failure with block gliding and even traces of earthflow appear on the images along parts of the larger fault zones that might have happened during more humid climate conditions than nowadays in the arid climate conditions (see also Figure 6). However, rare extreme recent weather events with high precipitation intensities causing flash floods might have similar impacts. Little is known about the intensity of the influence of flash floods on the surface expressions of geodynamic movements such as on pull-apart basins or flower structures.

The desert area of Egypt is often prone to sandstorms and, thus, to covers of aeolian sediments. Thus, especially radar data are useful tools for structural evaluations because of the penetration capabilities of radar signals into loose sedimentary covers.

4.1.3. Overview of Circular and Oval-Shaped Structures Situated between Larger Fault Zones Visible in Areas with Outcropping Cretaceous and Tertiary Sedimentary Layers

Movements along larger fault zones with different vertical and horizontal sizes and orientations, velocities and intensities can initiate rotations of the rocks between them, especially whenever larger fault zones intersect each other. Several processes like uplift, chemical diagenesis and overpressure turn rocks into over materials that exhibit brittle or ductile behavior. Brittleness and ductility of the different lithologic units is one of the key issues in the study of circular structures along fault zones in the Sinn El Kaddab Plateau and adjacent areas. Some of the oval-shaped and circular structures are related to rotation processes. The magnitude of the brittleness and ductility is determined by brittle mineral content (for example, quartz and feldspars) as well as the rock's mechanical properties [37]. Geomechanical inhomogeneities and discontinuities of the strata have the potential to disturb the stress field and cause deviations from the stress pattern (stress rotations). Ductile drag along the fault surface causes various forms of distortions and dislocations up to evidence for clockwise axis rotations. Which stress and amount and which properties can cause substantial stress rotations away from the material transition or a discontinuity have still to be investigated in this area.

The fact is that circular and oval-shaped structures surround the Sinn El Kaddab Plateau. The circular and oval-shaped structures are situated within lithologic outcrops of Tertiary (predominantly shales, marls, lime- and dolostones or sandstones).

Whereas at the eastern border circular structures are well pronounced in the topography, those in the western and southwestern parts are less distinct in the landscape. It can be observed that in the western border and the southwestern adjacent areas to the Sinn el Kaddab Plateau, some circular structures are larger than those along its eastern border. The circular and oval-shaped structures occur within lithologic outcrops of Tertiary shales, lime- and dolostones or sandstones. They were affected by later deformation processes, intersected and dislocated by predominantly E-W and N-S-striking fault zones, and by erosion. The height level at the center of these structures is often lower than the surrounding area which can be derived from DEM data.

Figure 19 provides an overview of these structures and their center points derived from evaluations of satellite images. Evaluations of remote sensing data can contribute to the discussion about the complex origin of these structures. Following explanations for the origin and development of these oval-shaped and circular structures might be possible:

- They might be the result of local uplifting processes up-doming the strata, thus, creating a circular pattern.
- The circular structures might be the result of dissolution processes in the lime and dolostones underneath, especially during past more humid climate conditions.
- They might be the result of rotation and compression processes along and between larger, active fault zones, especially in areas with predominantly outcropping shales.

The latter seems to be the most likely explanation. On Landsat and Sentinel 1-C-Band radar images, those circular structures become visible as well as on slope gradient maps and Landsat RGB mosaics (Figure 20). The RGB image (created by merging Sentinel 1 radar data with different radar polarizations) clearly shows several circular and oval-shaped structures with different sizes along fault zones. Amplified height level maps in a perspective view support the detection of detailed structures (Figure 21). Traces of both, ductile and brittle deformation could be observed on the satellite images. Traces of brittle deformation are characterized by a dense network of fractures visible as small lineaments. The arrangement of the homogeneous, ductile

deformation lines is parallel and equidistant. It seems that the rocks moved in the same direction and same distance, and their displacement field consisted of parallel vectors of equal length. The asymmetric shape of larger, oval-shaped structures in the W-E direction and the intersection with active fault zones striking E-W and SW-NE as shown in Figures 20–22 is evident. A clockwise rotation is assumed and partial folding. Small-scale fault block rotations may occur on any axis (vertical, horizontal, etc.).

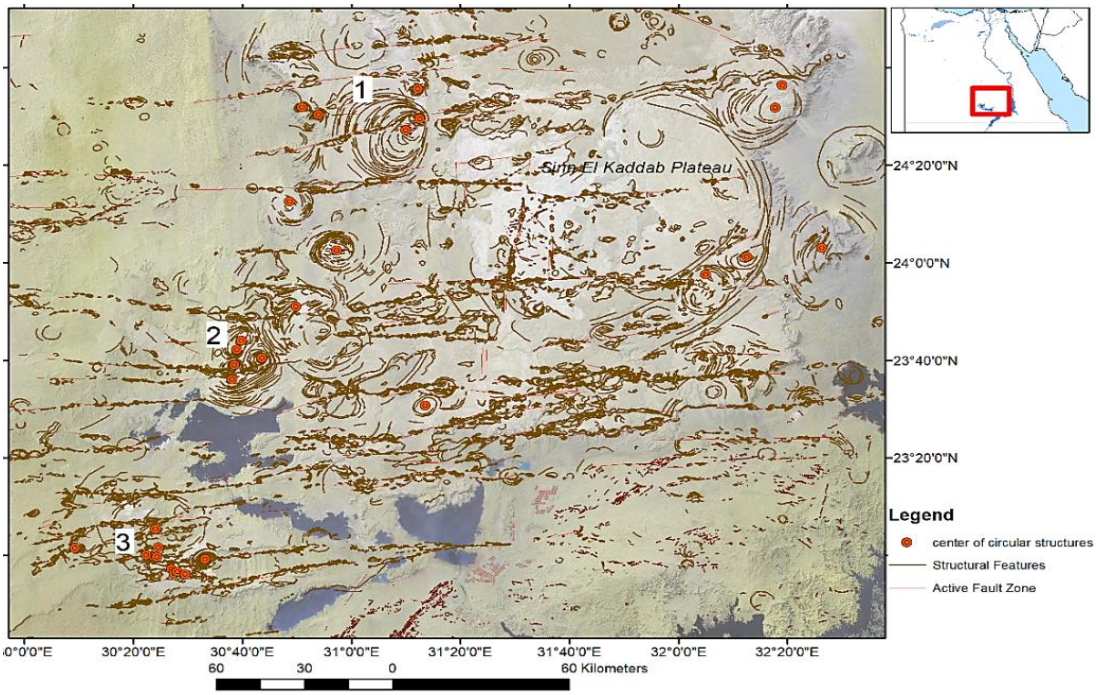

Figure 19. Overview of the oval-shaped and circular structures and their center points. 1–3 numbered areas are presented in the next figures.

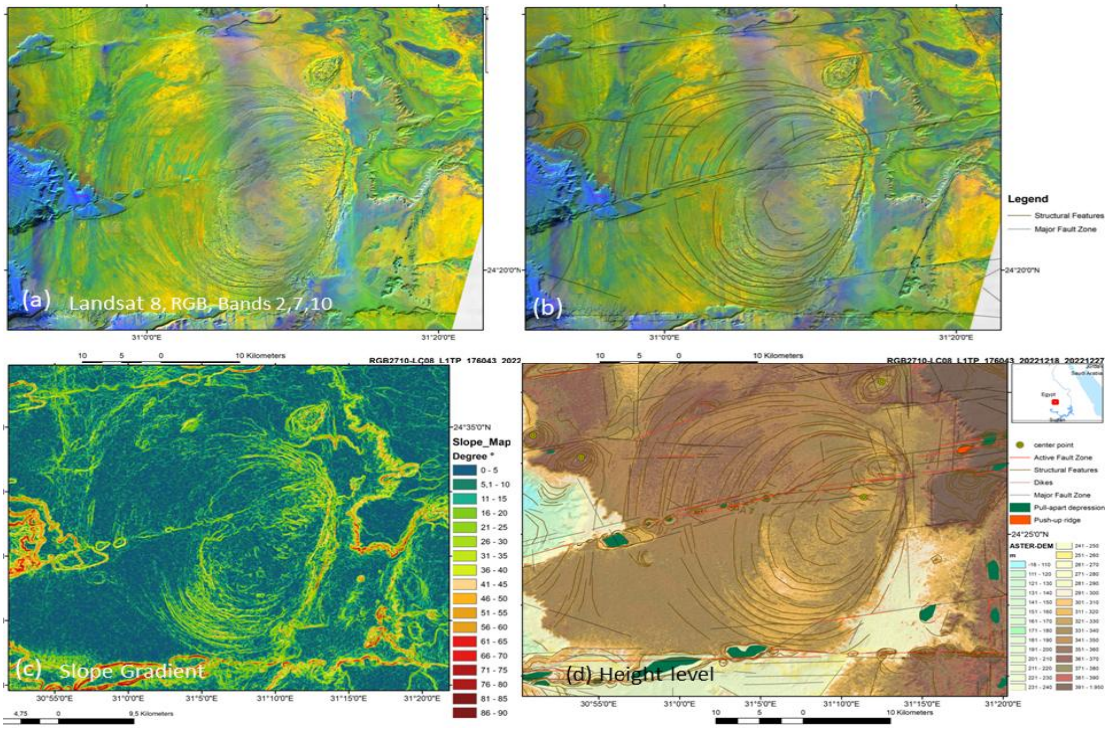

Figure 20. Oval-shaped structure (1 in Figure 19) is visible. (**a**) A Landsat scene; (**b**) A Landsat scene; (**c**) A slope gradient map; (**d**) A height level map.

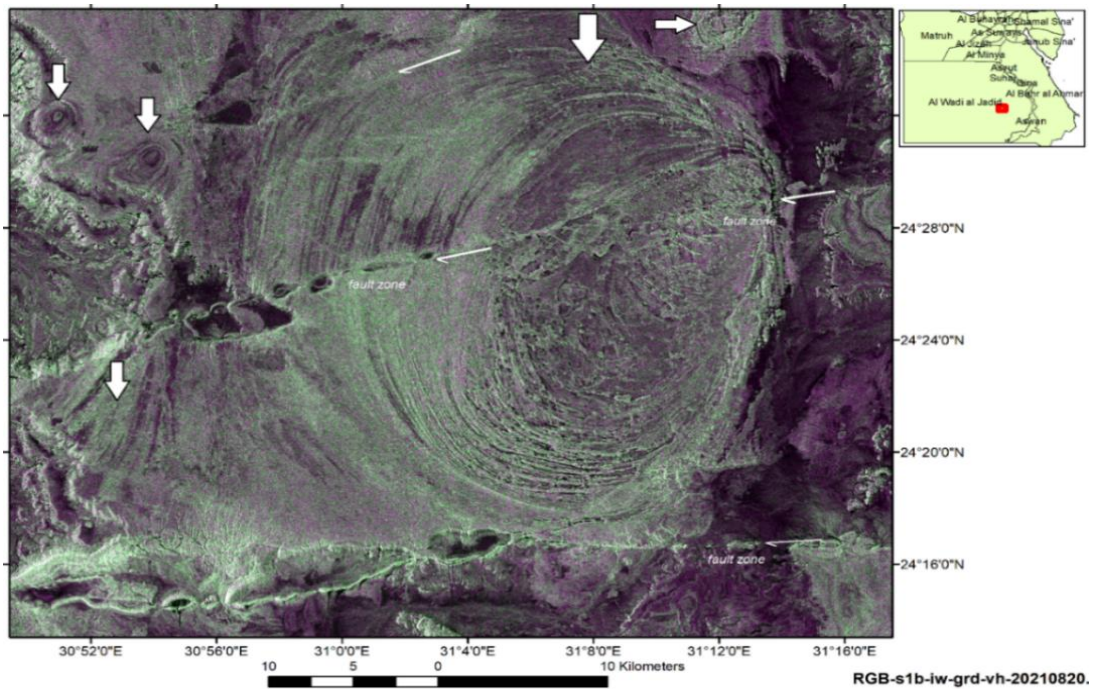

Figure 21. Sentinel 1 radar scene of oval-shaped structures (see position in Figure 19, 1). The larger white arrows indicate oval-shaped structures (the largest with a diameter of about 30 km in E-W-direction), the smaller, thinner white arrows the fault zones with push-up-ridges and pull-apart depressions.

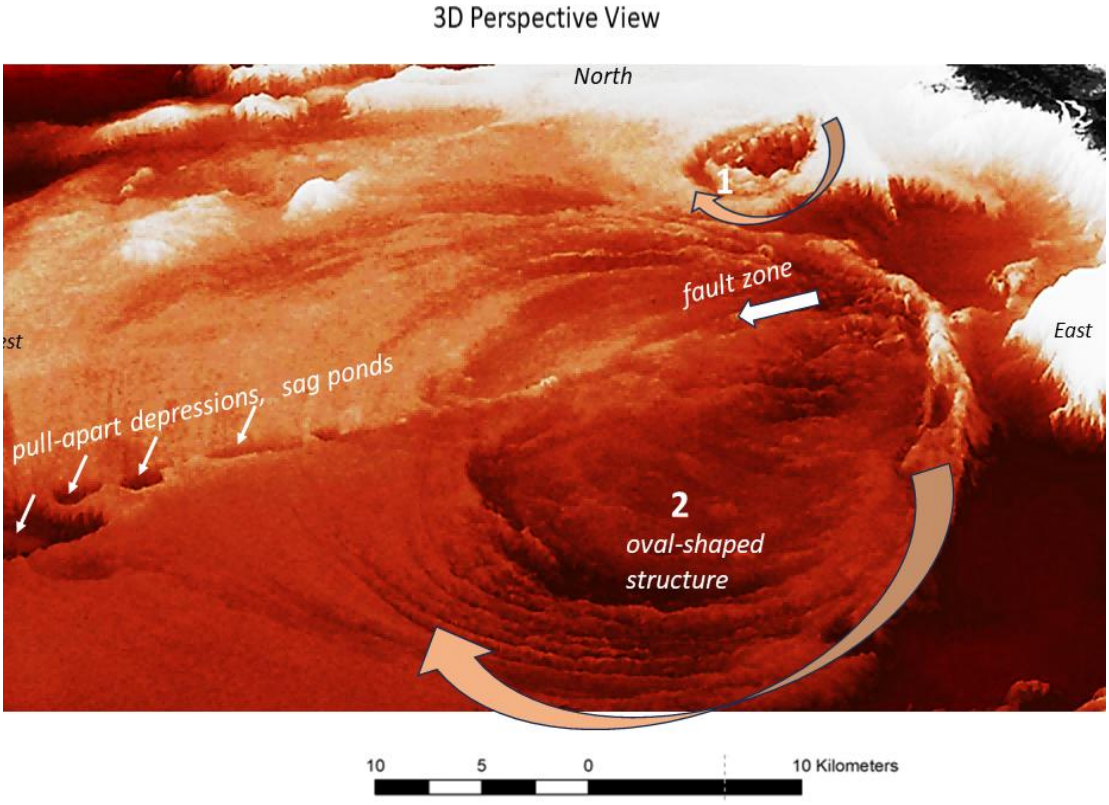

Figure 22. 3D perspective view (directed towards north) of the height level map (20 x amplification of the ALOS PALSAR DEM) showing oval-shaped structures assumed to be created by rotation movements. Orange arrows indicate the assumed clockwise rotation direction.

As strata underneath the surface with different lithological properties provide geomechanically inhomogeneities and discontinuities, they have the potential to influence the local stress field [26]. Which stress and amount and properties can cause substantial stress rotations away from the material transition or a discontinuity has still to be investigated in this area.

When analyzing the contours and shape of the oval- and circular-shaped structures on a Sentinel 1 RGB image (Figure 23e) a 5–10 km wide valley oriented in SSW-NNE direction becomes visible at their eastern border (orange lines in Figure 23f) as indicated by white arrows in Figure 23f. The outline of the eastern border of the complex with the oval- and circular-shaped structures fits very well with the corresponding outline of scarps on the opposite side of the valley at the western border of the Sinn El Kaddab Plateau like a puzzle piece. An amplification of this areas as presented in Figure 23g visualizes this very clearly. Thus, the valley appears to be a rupture and rift zone. The whole complex of circular structures was separated from the eastern rock units and moved about 5–10 km towards the west creating the rifting valley area. These westward movements supported rotation and folding processes. The circular and oval-shaped features are assumed to be created by clockwise rotations of the more ductile strata (shales, marls, limestones).

Besides the circular and oval-shaped structures traces of folding can be detected along and between larger fault zones. Figure 24 shows such a folding structure in more detail. The fold axis is oriented in the SW-NE direction.

At the western border of the Sinn El Kaddab Plateau, the circular and oval-shaped structures seem to be concentrated along an SSW-NNE-oriented zone (Figures 25a,b). Parts of the oval-shaped and circular structures are missing (derived from the interruptions in the contours of the structural lines) due to the dextral strike-slip movements along the faults, erosion and westwards movements. There are no traces of the missing part visible on the satellite images. These parts may have been sliced off (Figures 25 and 26).

Larger E-W- and WSW-ENE- striking fault zones are intersecting and displacing the circular structures. Therefore, they must be younger than these structures.

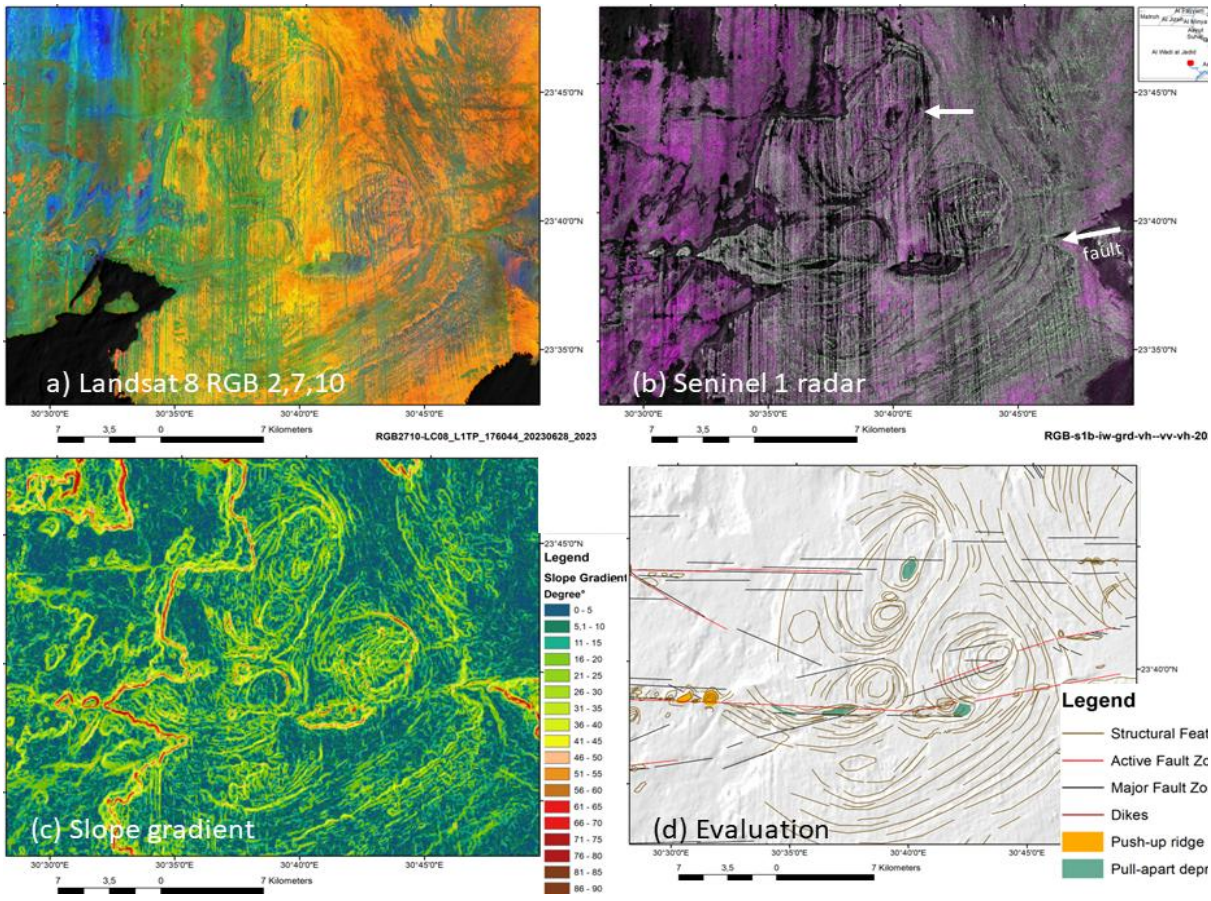

(a-d)

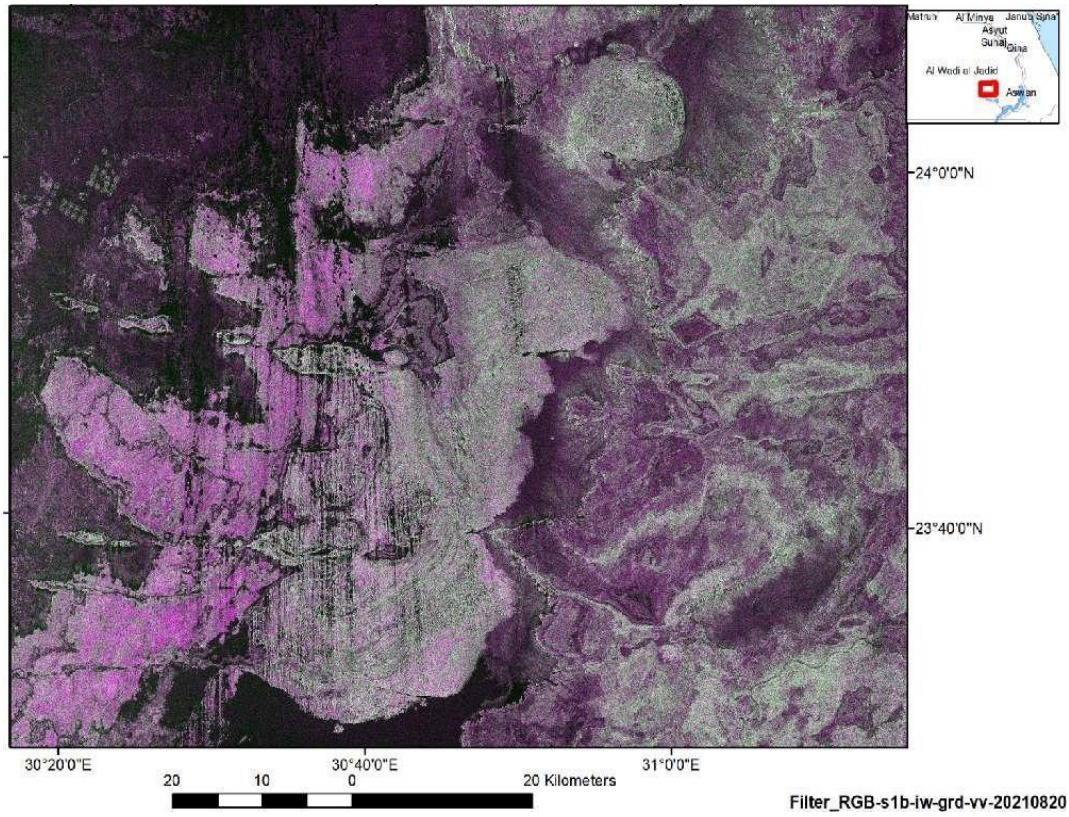
Matruh
Al Minya
Janub Sina'
Asyut
Suhaj
Qina
Al Wadi al Jadid
Aswan
24°0'0"N
23°40'0"N
30°20'0"E
30°40'0"E
31°0'0"E
20
10
0
20 Kilometers
Filter_RGB-s1b-iw-grd-vv-20210820

(e)

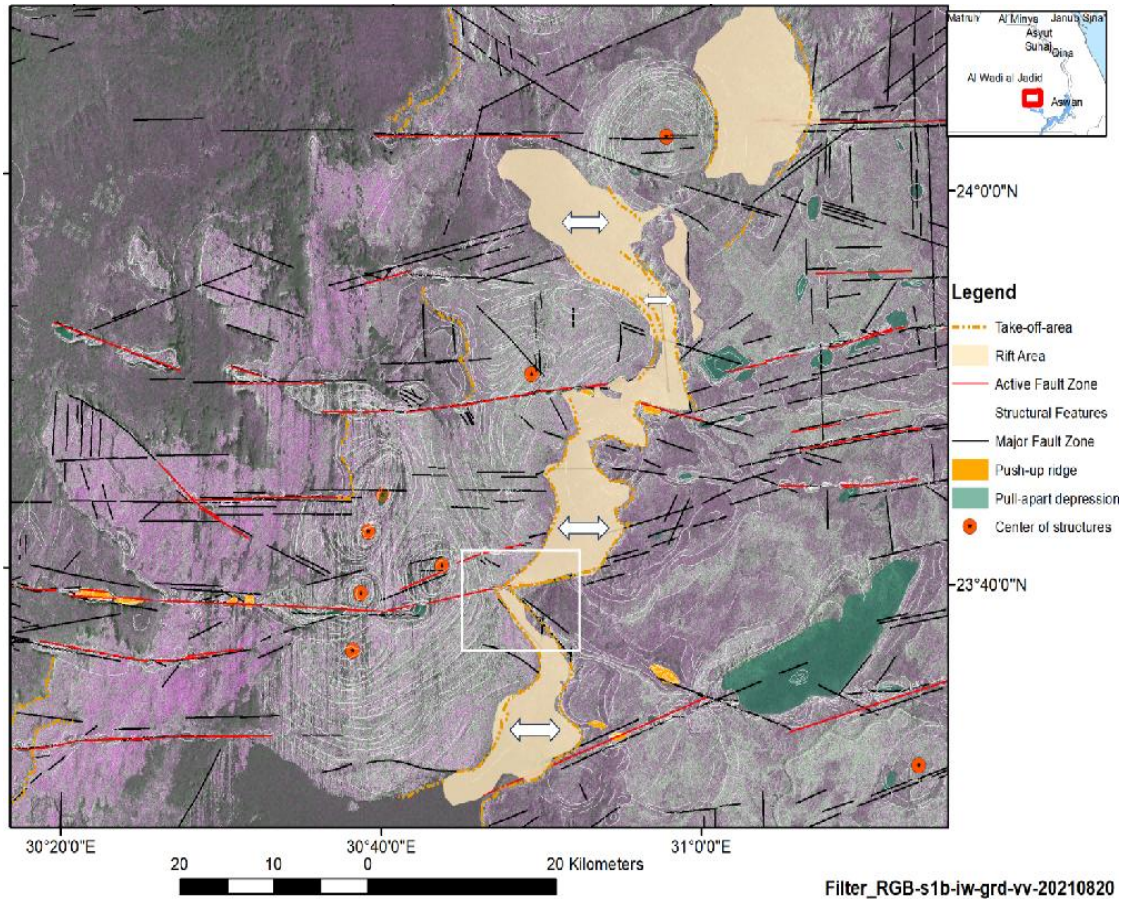
Matruh
Al Minya
Janub Sina'
Asyut
Suhaj
Qina
Al Wadi al Jadid
Aswan
24°0'0"N
23°40'0"N
Legend
Take-off-area
Rift Area
Active Fault Zone
Structural Features
Major Fault Zone
Push-up ridge
Pull-apart depression
Center of structures
30°20'0"E
30°40'0"E
31°0'0"E
20
10
0
20 Kilometers
Filter_RGB-s1b-iw-grd-vv-20210820

(f)

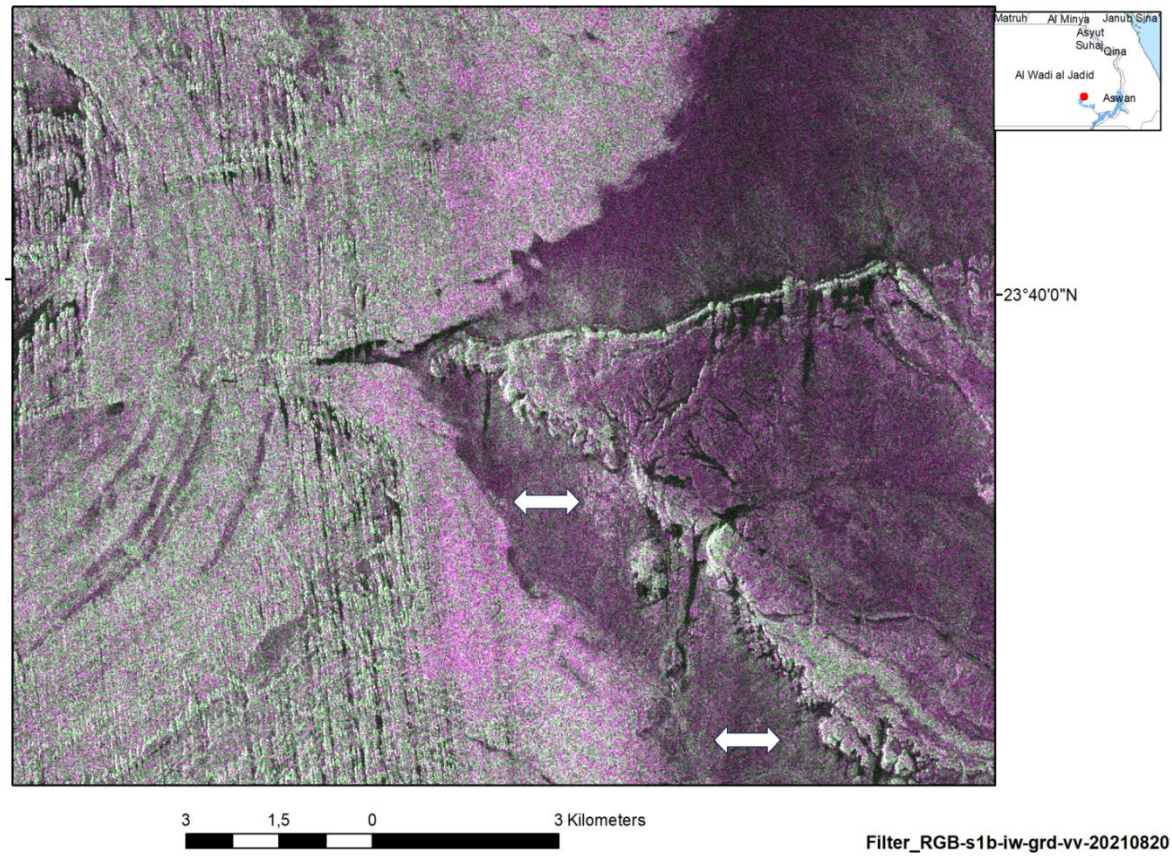

(g)

Figure 23. Circular and oval-shaped structures. (**a**) A Landsat 8-scene (2 on Figure 19); (**b**) A Sentinel 1 radar image (RGB image created by combining different polarizations: vh, vv, vh); (**c**) A slope gradient map; (**d**) The structural evaluation; (**e**) Sentinel 1 satellite radar image indicating ductile deformation patterns (rotation, folding); (**f**) Structural evaluation. The white arrows indicate the valley created by a rupture zone (rifting area); (**g**) Amplification of the indicated area is shown in Figure 23f of the rifting area separating the rock units. The white arrows indicate the moving direction.

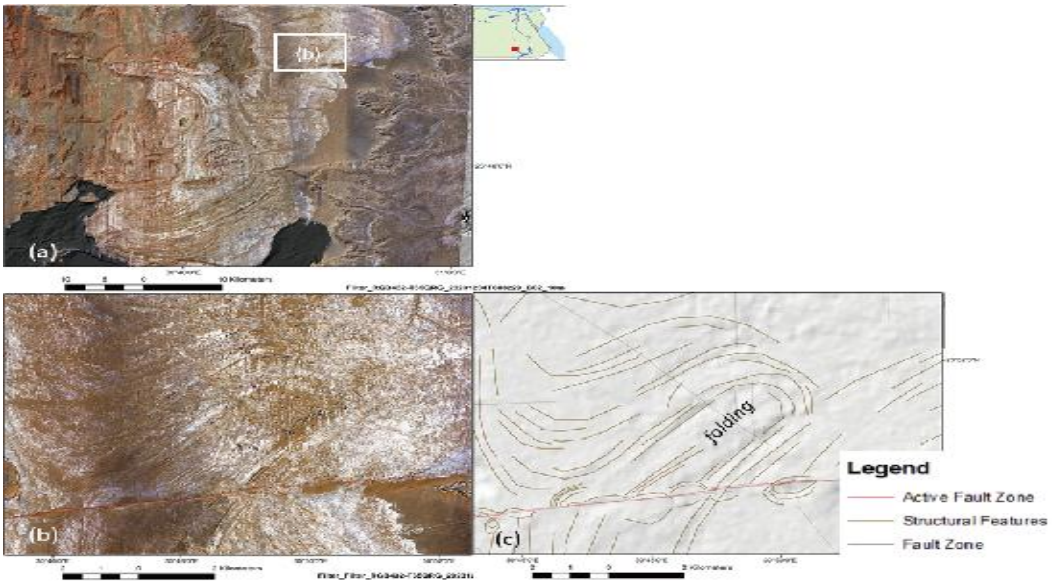

Figure 24. Sentinel 2 scenes and structural evaluation of the satellite data showing traces of folding. (**a**) Sentinel 2-scene; (**b**) Amplification of the Sentinel 2-scene to show the folded structure; (**c**) Structural evaluation.

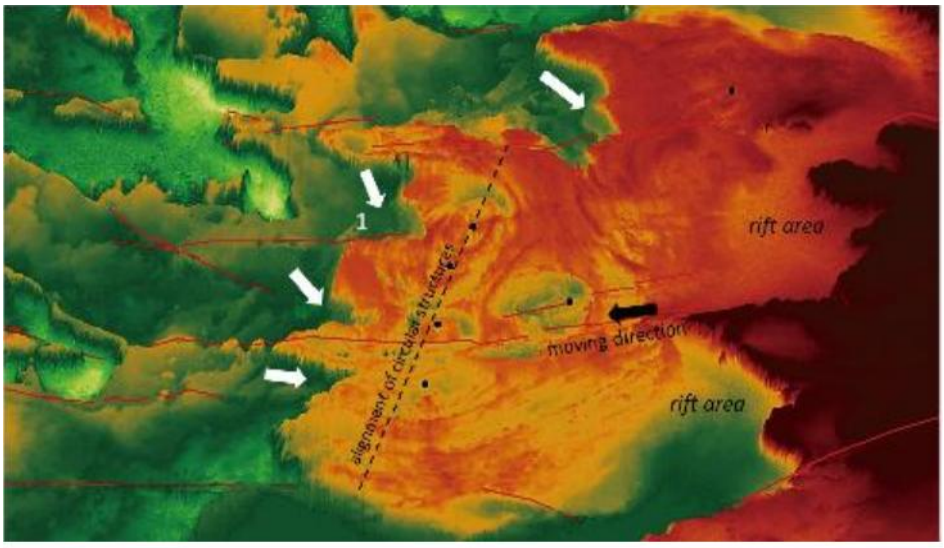

Parts of the structures missing

Central point of oval shaped structures

Active laull zone

(a)

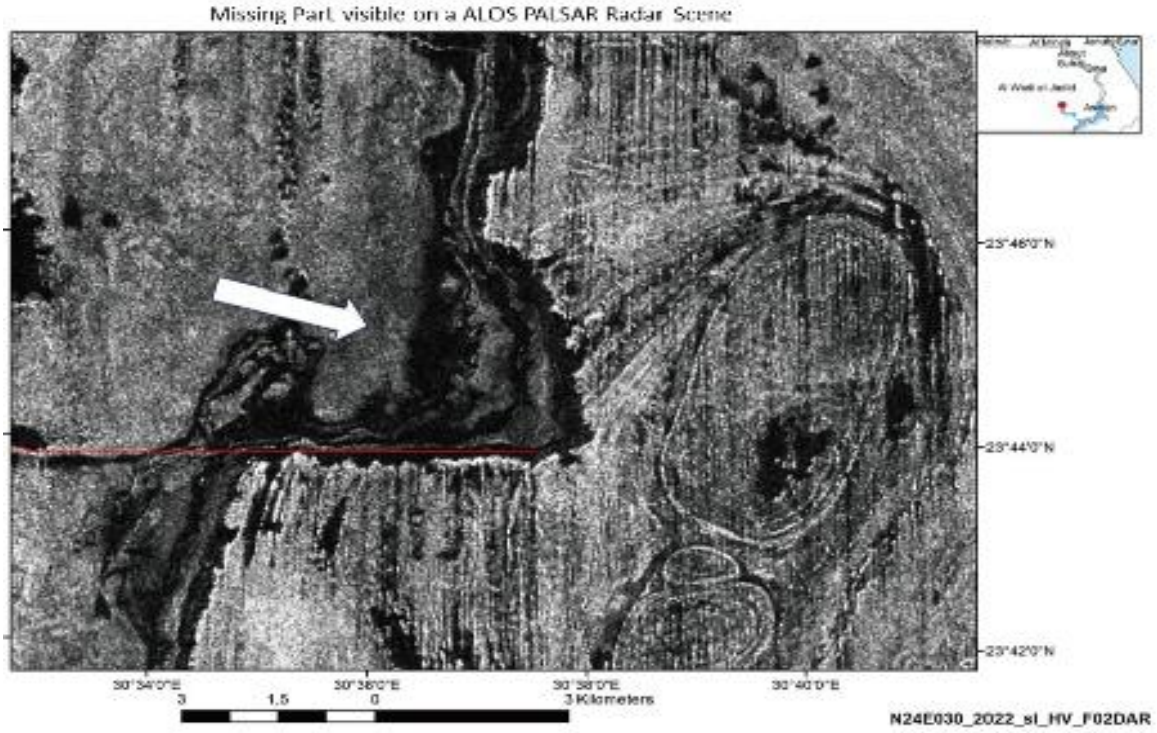

(b)

Figure 25. Traces of geodynamic activity. (**a**) 3D perspective view of the height level map based on ALOS PALSAR DEM data looking towards north) of the western Sinn el Kaddab Plateau and southwestern adjacent areas. The white arrows indicate missing parts of the structures; (**b**) ALOS PALSAR radar scene indicating a missing part of an oval-shaped structure (Figure 25a, area 1).

Figure 26 shows an example of a rotated and dislocated block between larger fault zones. The rotated complex is missing its western part.

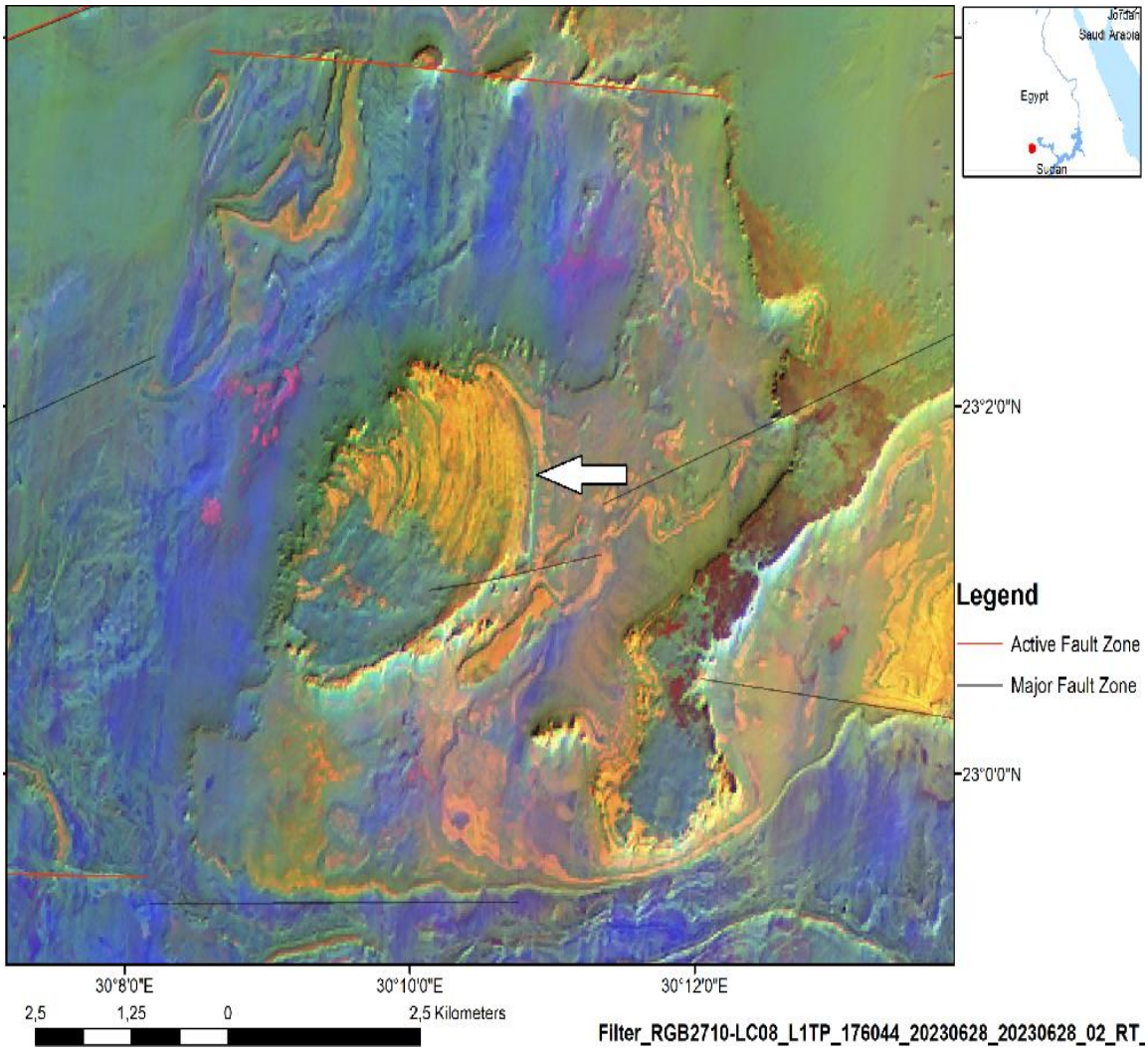

Figure 26. Rotated and displaced rock complex visible on a Landsat 8 RGB scene. This block has been transported towards the southwest from its original site of origin as indicated by the white arrow. The movement dynamics obviously have been influenced by the position of larger fault zones (black and red lines).

Figure 27 provides examples of smaller circular features that have been affected by active strike-slip fault zones. Whether they are the result of the dissolution process in limestones or of rotation processes cannot be answered by remote sensing methods. The smaller circular structures seem to be the result of rotation movements along and between active dextral strike-slip fault zones (Figure 27).

Deformations and movements of the southern part of a ring structure towards the west are visible in the next example in Figure 28, obviously related to the dextral strike-slip movements of the intersecting fault zone. Similar structures were observed by [32].

When analyzing the occurrence and distribution of the circular and oval-shaped structures with height level data, it is obvious that the structures are concentrated in height levels between 190–340 m in the western part of the Sinn El Kaddab Plateau, whereas in the eastern and southeastern part, they are situated above 400 m. The circular structures in the west occur concentrated in the SSW-NNE direction in the transition zone between the locally lowest areas below 120 m and the higher areas of the Sinn El Kaddab Plateau above 400 m.

The question arises of whether height differences influenced rock instability and rock deformation. Are there gravity-driven deformation of sedimentary strata involving downslope-directed movement?

Is the current topography related to deeper crustal structures or a westward dip of the strata? The concentration of circular structures in an SSW-NNE direction (Figure 25) along the western border of the Sinn El Kaddab Plateau might have been affected by the crustal structure and its ongoing geodynamic movements.

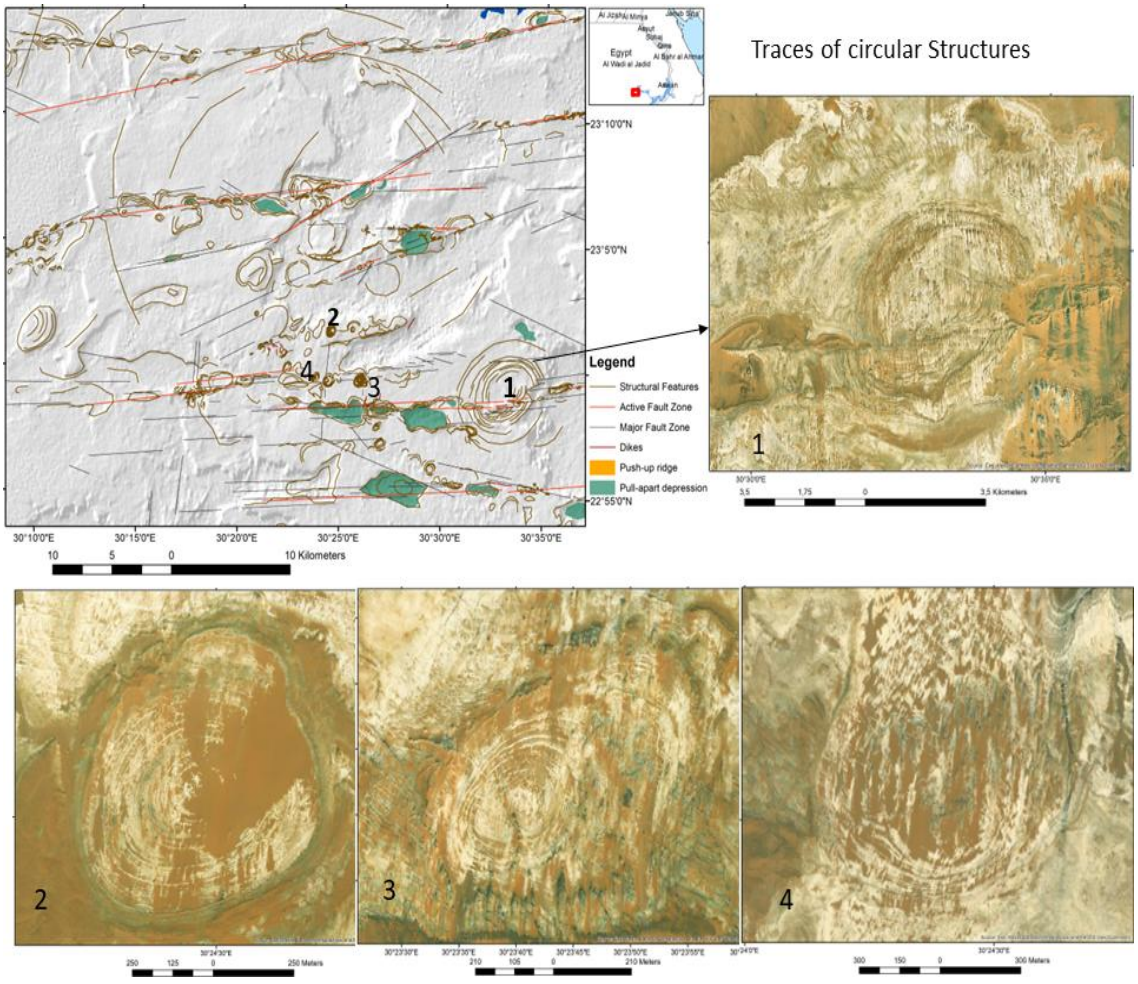

(a)

(b)

Figure 27. Mapping of fault related circular structures. (**a**) Traces of circular structures on satellite scenes (World Imagery/ESRI) aligned along larger, E-W-striking fault zones (area 3 on Figure 19); (**b**) Structural evaluation.

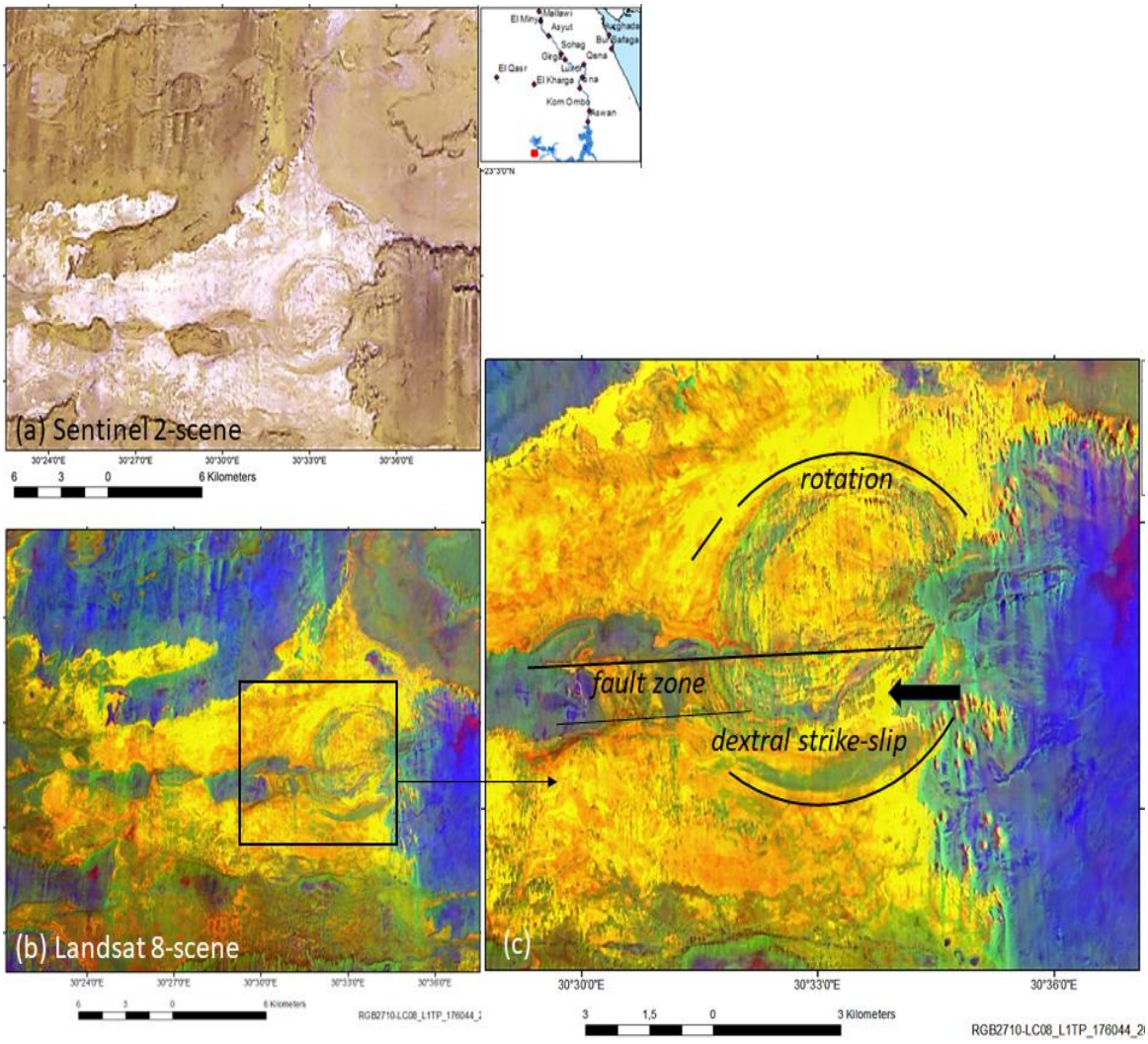

Figure 28. Depressions and potential block rotation along the Seiyal fault. (**a**) Sentinel 2; (**b**) Landsat 8-scenes; (**c**) simplified illustration of the possible dextral strike–slip. The southern parts are partly displaced towards the west.

Crustal properties-related information can be derived from the CPD map of this area derived from aeromagnetic data as shown in Figure 29. By estimating the CPD knowledge of the thermal structure of the crust can be inferred. (The Curie point depth, CPD, is the depth in the Earth's crust at which ferromagnetic minerals are converted into para-magnetic minerals due to an increase in the temperature.) The shallowest CPDs are associated with crustal thinning [38,39]. The CPDs range from 8.6 to 35.7 km with an average value of 20 km.

In the west of the Sinn el Kaddab Plateau the areas with the lowest (from the surface point of view) CPD depth values (>26 km, dark-blue on the lower map in Figure 29a) correspond to the lowest topographic regions at the surface (<120 m, dark-green in Figure 29b). The lowest area below 120 m height level is forming depressions like the Kharga Oasis depression in the SSW-NNE direction nearly parallel to the rifting area. Whether there is a geodynamic relationship like subsidence or rifting between the lower CPD depth position and the lower surface topography has still to be investigated. However, it seems likely. Underneath the Sinn El Kaddab Plateau, the CPD depth is estimated to be in less than 20 km. Several authors described uplifting movements in the Sinn el Kaddab Plateau [10,22]. These uplifting movements could have intensified faulting and block-wise rotations.

As a contribution to the monitoring of potential damages caused by active faults that might be prone to long-term creeping movements or might be affected by strong motions because of earthquakes, the digitized

faults were merged with road and railroad shapefiles [3]. The intersection of roads and railroads with fault zones was pointed out (Figure 30). The knowledge of intersection points might support the focused maintenance of the infrastructure.

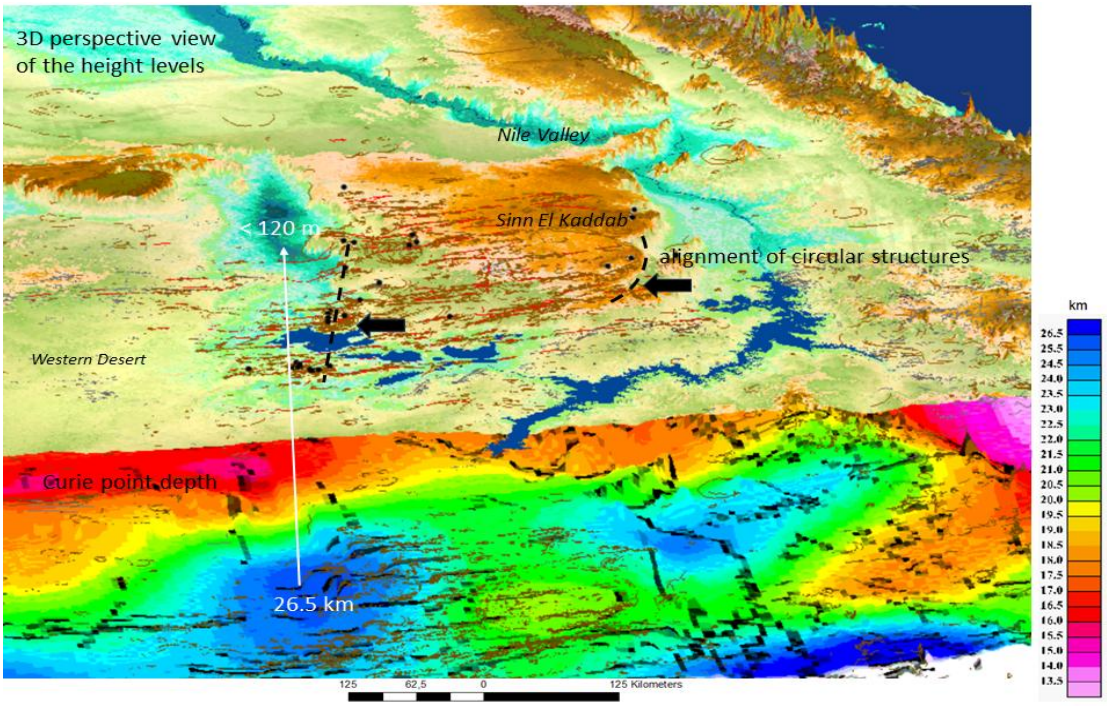

(a)

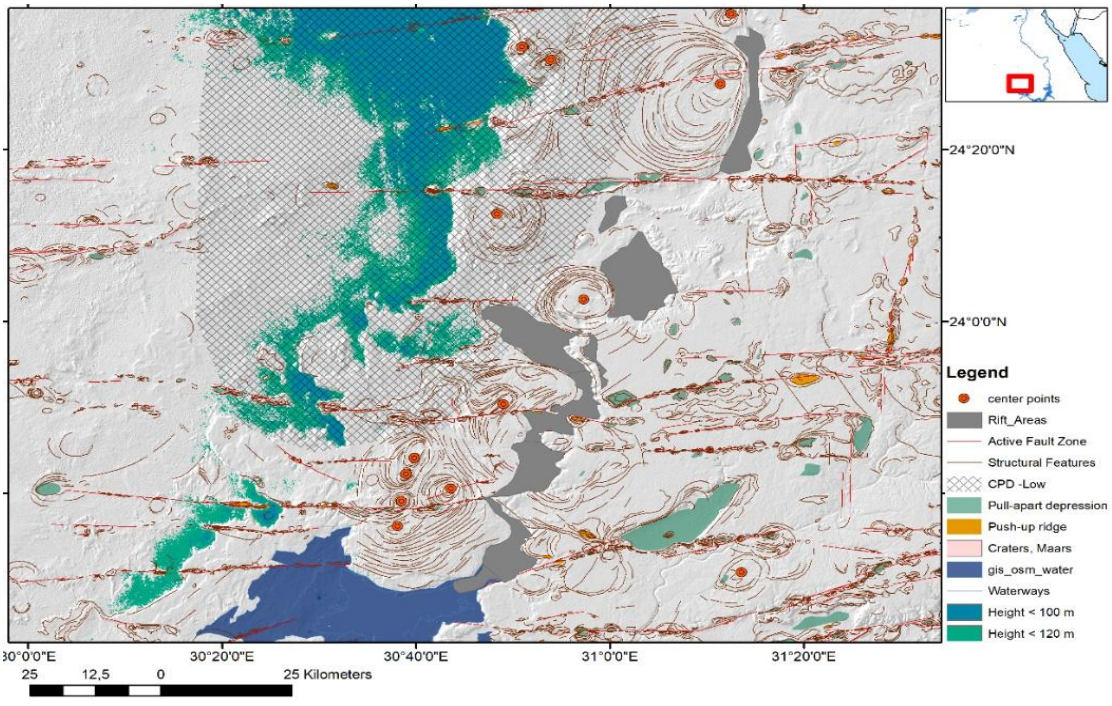

(b)

Figure 29. Combining topographic data with CPD information. (**a**) 3D perspective view of the height level map (above, looking north) and the Curie Point Depth (CPD) Map [38], (below) merging the maps with ASTER DEM Data. The use of the CPD map was permitted by the authors. The structure lines, derived from the geological map on scale 1:2000000, Geological Survey of Egypt [20], are overprinted on the map. Digitized fault zones (red lines) are included in (b); (**b**) The areas with the lowest (from the surface point of view) CPD values (>20 km)

correspond to the lowest topographic areas (<120 m).

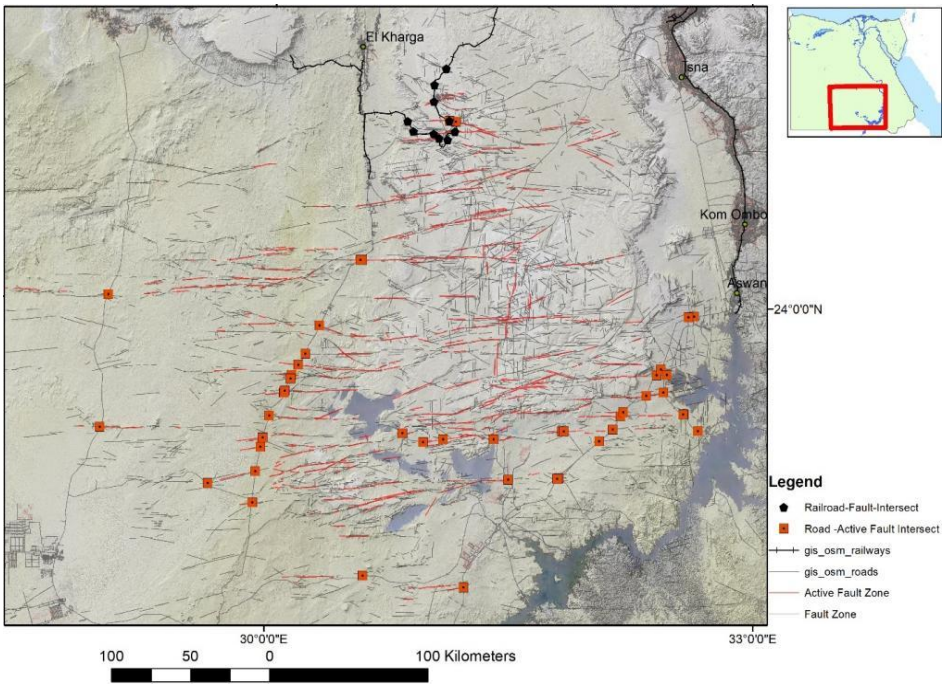

Figure 30. Intersection points of active fault zones crossing roads and railroads.

4.2. Fault Zones in the Western Desert

The development and density of fault-related structures are less expressed in the Western Desert than in the Sinn el Kaddab plateau because of differences in the lithologic properties of the host rocks with prevailing sandstones (Figure 31). Prominent fault zones in the Western desert show a different appearance in comparison with those in the Sinn El Kaddab Plateau. They are characterized by an increasing influence of traces of magmatic activity from E to W, less ductility and more brittleness. Many faults are visible on satellite images because of narrow intrusions of dikes [40,41]. The faults show long, parallel segments oriented in ESE-WNW and SSW-NNE directions, associated with complex, deformation zones of subsidiary faults, step-overs and *en échelon* folds. Based on surface geology, and geophysical data, it is evident that the southern part of the Western Desert is controlled mainly by the Nubian Fault System (NFS). The majority of the NFS are mainly pre-existing E-W striking strike-slip faults [27,42,43].

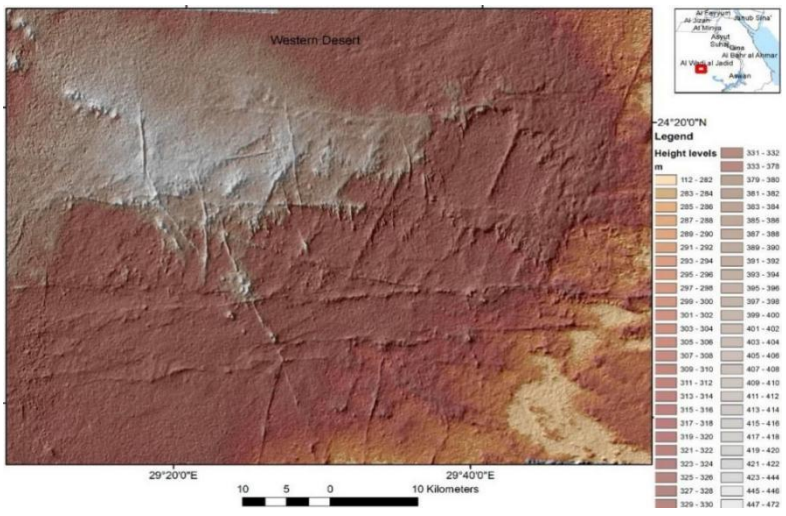

(a)

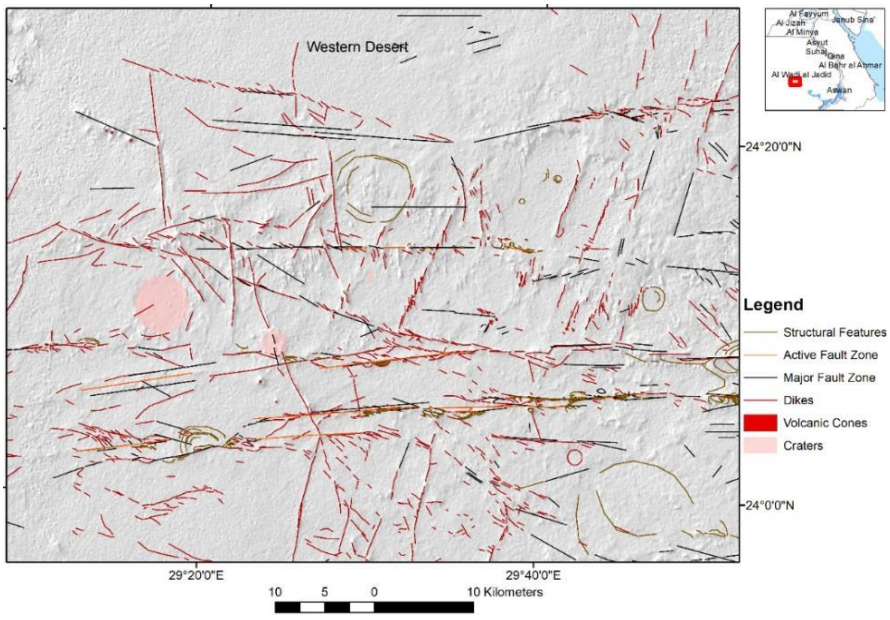

(b)

Figure 31. Parallel fault segments with Riedel shear zones, dike intrusions and craters. (**a**) On a height-level map; (**b**) On the evaluation map.

The next Figure 32 demonstrates the use of radar data for the detection of faults and fault-related structures that are not visible on optical satellite images due to the coverage with aeolian sediments. Traces of faults and their related deformation structures can be mapped based on the radar images and, thus, additional knowledge gained. Sag ponds and rock lenses are aligned along the fault zone oriented in the ESE-WNW direction in SW-Egypt (Figure 32a). The large sprinkler irrigation field is bordered in the south by these fault segments (Figure 32b). When planning and monitoring the irrigation network, this fault zone has to be considered.

Sprinkler irrigation planning is a complex task that includes the awareness of active fault systems or the effects of earthquakes to avoid damage to the irrigation network and sprinkler systems. Traces of magmatic activity such as dikes, plugs or craters have to be considered as well as they form hindrances for irrigation systems as demonstrated in Figure 33.

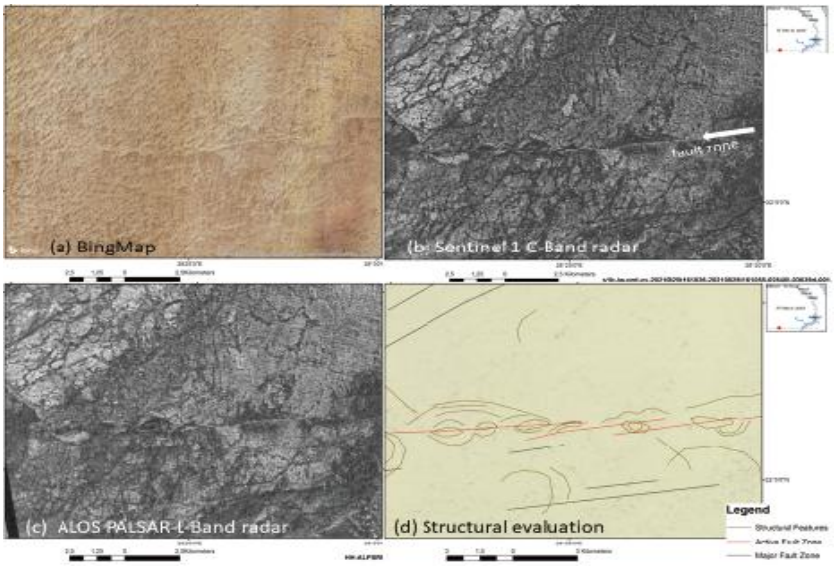

(a)

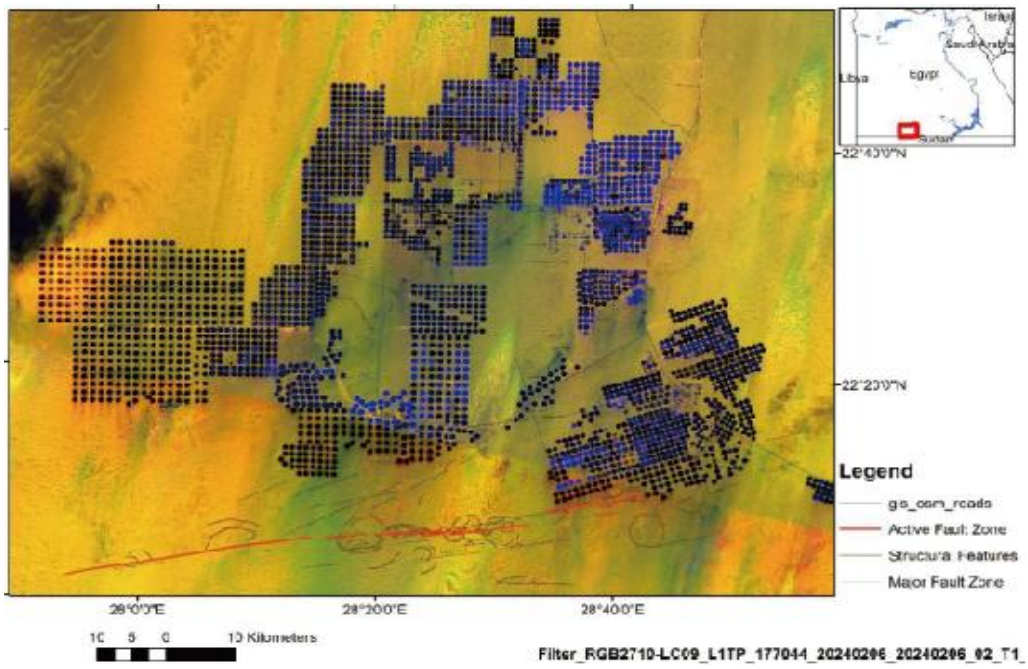

(b)

Figure 32. Fault zone in an irrigation area. (**a**) The detection of fault zones on radar data in the south of the irrigation field is shown below; (**b**) Sprinkler irrigation field in S-Egypt visible on a Landsat 9 RGB-scene (acquisition date: 06.02.2024) bordered in the south by a WSW-ENE striking fault as detected on radar images shown in (a).

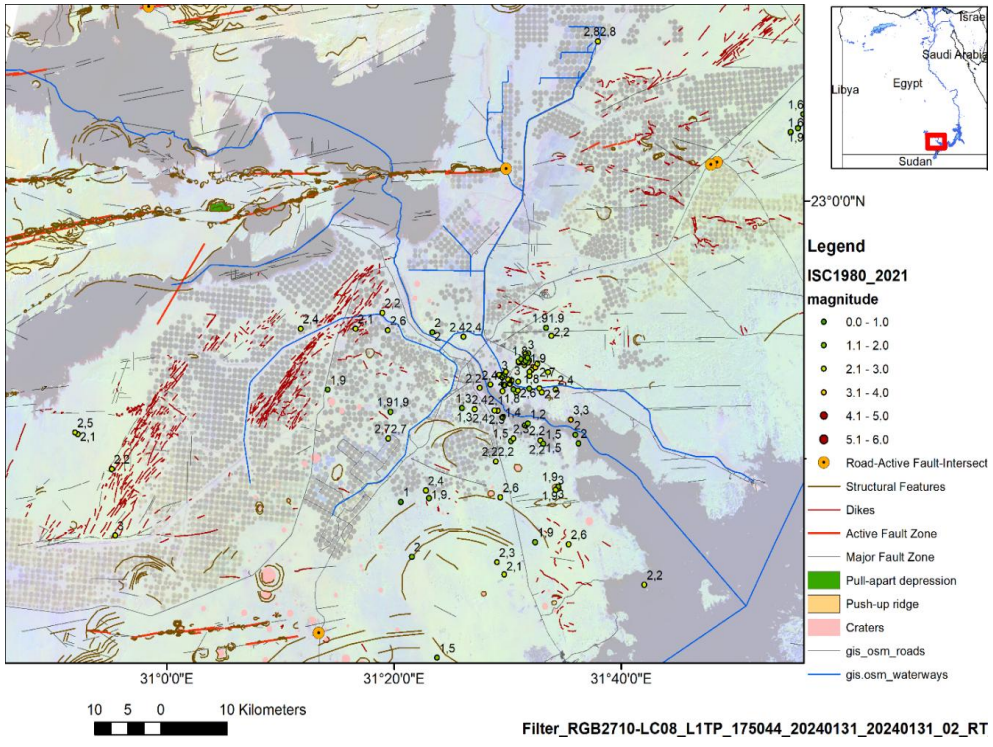

Figure 33. Georisks affecting the surveillance and maintenance of sprinkler irrigation fields in southern Egypt (active fault zones, earthquakes, dikes, plugs, craters).

5. Discussion

Remote sensing has proven its value for the 2D detection of fault zones and fault-related structures and their deformation pattern in Egypt. Around the Sinn El Kaddab Plateau large circular and oval-shaped structures between the different active, mainly E-W, N-S and SW-NE oriented fault zones can be observed. The circular and oval-shaped features along the western border of the Sinn El Kaddab Plateau are assumed to be partly the result of block rotation in shales, marls and limestones between the predominantly W-E and N-Soriented, larger fault zones. Further research should be carried out in the future to investigate the origin of these structures.

Displacements of single blocks, separated from the circular structures, are observed. Only some of them can be traced on the satellite images, others might be covered by eolian sediments. Little is known so far about the age and period of these movements and the movement intensities.

The observed rift valley at the western border of the Sinn El Kaddab Plateau has not yet been described in the available literature, although the matching contours of the valley borders are obvious. This rift valley should be monitored by geodetic measurements and geophysical surveys to learn more about the rifting processes and their velocities.

The overview of fault zones in Southern Egypt leads to even more questions. For example, many questions are still open with regard to the kinematics and interactions of faults such as in areas of intersecting of larger fault zones.

In the case of stronger earthquakes, larger and wider fault zones might have an impact on seismic wave propagation by forming asperities and barriers, of course depending on the strike, dip, width and depth of the faults. There are multiple reflections and constructive interference of seismic waves at the boundaries of faults, especially after dike intrusions into fault zones, thus, amplifying the local effects of earthquakes. The impact of fault zones on local site conditions influencing ground motion surely needs further investigation.

6. Conclusions

Ground-surface deformation hazards associated with active faults such as faulting and folding within a deformation zone should be monitored carefully. An active fault is likely to have renewed displacement in the future. The overview of faults and fault-related deformation structures based on the evaluation of satellite data and geologic maps contributes to the knowledge of fault geometries, fault orientation changes (turns, bends), stepovers, separations, or discontinuities.

Structural features were digitized as detailed as possible such as sag ponds, pull-apart basins as well as ridges in combination with digital terrain data. Of course, the use of remote sensing data comes to its limits whenever detailed 3D knowledge about the kinematics and structure of faults is demanded. Nevertheless, different types of faults and fault segments depending on the host rock properties could be identified.

The awareness, understanding and knowledge about fault zones and fault-related structures and the potential secondary effects after stronger earthquakes (abrupt vertical and horizontal displacements) is an important step towards land use planning aiming at the mitigation of risks and towards the monitoring and maintenance of infrastructure in Egypt such as the road and railroad network. In the case of surface-near, stronger earthquakes reactivating existing faults or creating new ones this might be of importance. The assessment of potential seismic hazards on segments of active faults is an important approach for long-term earthquake risk assessment as well.

The role of larger, active fault zones within and around the reservoir lakes has still to be investigated more in detail as shallow earthquake swarms that occurred during the last decades around the reservoirs, seem to be related to water intruding into the fault zones and, thus, to fluids triggering earthquakes. Moreover, pore pressure and fluid diffusion play an essential role in the fault activation process.

Fault hazard assessment could be improved by pooling data from different regions in Egypt, rather than basing predictions exclusively on local data. By systematic and standardized pooling and sharing of fault data from across Egypt in a GIS data base potential damage from movement along active faults can be better assessed and monitored. Such a database might be the starting point for the use of open-source WEB-based tools such as the tool PreventionWeb of UNDRR-disaster risk reduction community [44], the global knowledge-sharing platform for disaster risk reduction and resilience. It has channeled the solutions for robust and effective management and decision-making in multi-hazard risk.

Author Contributions

The author contributed to all the parts and aspects of this manuscript.

Funding

This work received no external funding.

Data Availability Statement

The sources of the used remote sensing data, GIS software and shapefiles are mentioned in the Material and Methods chapter, further on in the text and the references.

Acknowledgments

The author is grateful to the Editorial Team/Editorial Office of the Journal *Prevention and Treatment of Natural Disasters,* UK Scientific Publishing Limited, for all their support and efforts. The author is grateful for the efforts of the reviewers. Mrs.Verena Willige-Kottke/Munich, Germany, is kindly acknowledged for fruitful discussions and input of her ideas.

Conflicts of Interest

The author declares no conflict of interest.

References

1. Moustafa, S.S.R.; Abdalzaher, M.S.; Abdelhafiez, H.E. Seismo-lineaments in Egypt:Analysis and implications for active tectonic structures and earthquake magnitudes. *Remote Sens.* **2022**, *14*(23), 6151. [CrossRef]
2. Genidi, H.; Saleh, M.; Mohamed, A.M.; Othman, A.; El Mahmoudi, A. Recent estimates of the ground deformation from remote sensing and terrestrial data around the High Dam Area, Aswan, Egypt. *Egypt. J. Remote Sens. Space Sci.* **2023**, *26*(3), 403–414. [CrossRef]
3. Geofabrik's free download server for OpenStreetMap data. Available online: http://download.geofabrik.de/africa.html
4. Mohamed, A.E.A.; El-Hadidy, M.; Deif, A.; Elenean, K.A. Seismic hazard studies in Egypt. *NRIAG J. Astron. Geophys.* **2012**, *1*(2), 119–140. [CrossRef]
5. Saadalla, H.; Abdel–aal, A.A.K.; Mohamed, A.; El-Faragawy, K. Characteristics of earthquakes recorded around the high dam lake with comparison to natural earthquakes using waveform inversion and source spectra. *Pure Appl. Geophys.* **2020**, *177*, 3667–3695. [CrossRef]
6. Trinh, P.; Vinh, H.; Huong, N.; Liem, N. Active fault segmentation and seismic hazard in Hoa-Binh reservoir, Vietnam. *Cent. Eur. J. Geosci.* **2013**, *5*(2), 223–235. [CrossRef]
7. Global Active Faults Database (GEM GAF-DB). Available online: https://blogs.openquake.org/hazard/global-active-fault-viewer/
8. Styron, R.; Marco Pagani, M. The GEM global active faults database. *Earthq. Spectra.* **2020**, *36*(1_suppl), 160–180. [CrossRef]
9. Jerris, T.J. Development of structural basins and domes on the Sinn El-Kaddab Plateau, Egypt: insights from in situ data and application of moderate resolution orbital imagery of the Seiyal Fault. Master's thesis, Missouri University of Science and Technology, Rolla, 2014.
10. Hamimi, Z; Hagag, W.; Osman, R.; El-Bialy, M.; Abu El-Nadr, I.; Fadel, M. The active Kalabsha Fault Zone in Southern Egypt: Detecting faulting activity using field-structural data and EMR-technique, and implications for seismic hazard assessment. *Arab. J. Geosci.* **2018**, *11*, 421. [CrossRef]
11. Rashwan, M.; Sawires, R.; Radwan, A.M.; Sparacino, F.; Peláez, J.A.; Palano, M. Crustal strain and stress fields in Egypt from geodetic and seismological data. *Remote Sens.* **2021**, *13*(7), 1398. [CrossRef]
12. El Bohoty, M.; Ghamry ,E.; Hamed, A.; Khalifa, M.; Taha, A.; Meneisy, A. Surface and subsurface structural mapping for delineating the active emergency spillway fault, Aswan, Egypt, using integrated geophysical data. *Acta Geophys.* **2023**. [CrossRef]
13. Bauer, H.; Rogowitz, A.; Habler, G.; Grasemann, B.; Decker, K. Interaction of frictional and plastic deformation mechanisms in a clay-carbonate strike-slip fault (Northern Calcareous Alps, Austria). *J. Struct. Geol.* **2023**, *166*, 104774. [CrossRef]

14. JAXA/METI, satellite data accessed through ASF DAAC. Available online: https://www.asf.alaska.edu/ (accessed from May to September 2023).
15. Paillou, P. Mapping palaeohydrography in deserts: Contribution from space-borne imaging radar. *Water.* **2017**, *9*(3), 194. [CrossRef]
16. Earth Explorer. Available online: https://earthexplorer.usgs.gov/ (accessed from May 2023 to January 2024).
17. ESA Copernicus Open Access Hub. Available online: https://dataspace.copernicus.eu/
18. JAXA, PALSAR-2 Global Forest/Non-forest Map "2022". Available online: https://www.eorc.jaxa.jp/ALOS/en/palsar_fnf/data/2022/map.htm
19. Arab Nubia Group Blog, GIS, Remote Sensing & General, Applications. Available online: https://blog.arabnubia.com/
20. Geologic Map of Egypt, 1981, 1: 2 Mio, Egyptian Geological Survey and Mining Authority, Cairo, Egypt. Available online: https://esdac.jrc.ec.europa.eu/content/geologic-map-egypt
21. Geomorphic Evolution of The Kurkur-Dungul area in Response to Tectonic Uplifting and ClimaticChanges, South Western Desert, Egypt. Available online: https://www.academia.edu/53375547/Geomorphic_Evolution_of_The_Kurkur_Dungul_area_in_Response_to_Tectonic_Uplifting_and_Climatic_Changes_South_Western_Desert_Egypt
22. Alrefaee, H.A. Crustal modeling of the central part of the Northern Western Desert, Egypt using gravity data. *J. Afr. Earth Sci.* **2017**, *129*, 72–81. [CrossRef]
23. Sakran, S.; Said, S.M. Structural setting and kinematics of nubian fault system, se western desert, Egypt: An example of multi-reactivated intraplate strike-slip faults. *J. Struct. Geol.* **2018**, *107*, 93–108, [CrossRef]
24. Saleh, S.; Pamukcu, O.; Brimich, L. The major tectonic boundaries of the Northern Red Sea rift, Egypt derived from geophysical data analysis. *Contrib. Geophys. Geod.* **2017**, *47*(3), 149–199. [CrossRef]
25. Saleh, M.; Masson, F.; Mohamed, A.M.S.; Boy, J.P.; Abou-Aly, N.; Ali Rayan, A. Recent ground deformation around lake Nasser using GPS and InSAR, Aswan, Egypt. *Tectonophysics.* **2018**, *744*, 310–321. [CrossRef]
26. Zhang, S.; Ma, X. How does in situ stress rotate within a fault zone? Insights from explicit modeling of the frictional, fractured rock mass. *J. Geophys. Res.: Solid Earth.* **2021**, *126*(11), e2021JB022348. [CrossRef]
27. Tewksbury, B.; Mehrtens, C.J.; Gohlke, S.A.; Tarabees, E.A.; Hogan, J.P. Constraints from Mesozoic siliciclastic cover rocks and satellite image analysis on the slip history of regional E-W faults in the southeast Western Desert, Egypt. *J. Afr. Earth Sci.* **2017**, *136*, 119–135. [CrossRef]
28. ISC Bulletin: interactive event catalogue search. Available online: http://www.isc.ac.uk/iscbulletin/search/catalogue/interactive/
29. Earthquake data. Available online: https://earthquake.usgs.gov/earthquakes/search/ (accessed on 14 September 2023).
30. Earthquake data. Available online: http://www.emsc-csem.org/ (accessed on 20 September 2023).
31. Mohamed, A.S.; Hassib, G.H.; AbouAly, N.; El-Kutb, A. Evaluation of recent crustal deformation and seismicity in spillway fault area, Aswan, Egypt. *NRIAG J. Astron. Geophys.* **2022**, *11*(1), 325–336. [CrossRef]
32. Alam, A.; Ahmad, S.; Bhat, M.S.; Ahmad, B. Tectonic evolution of Kashmir basin in northwest Himalayas. *Geomorphol.* **2015**, *239*, 114–126. [CrossRef]
33. Atmaoui, N. Development of Pull-Apart Basins and associated Structures by the Riedel-Shear Mechanism: Insight from scaled Clay Analogue Models. Ph.D. thesis, Fakultät für Geowissenschaften der Ruhr-Universität Bochum zur Erlangung des Doktorgrades der Naturwissenschaften, Bochum, 2005.
34. El Aala, A.K.A.; Nabawyc, B.S; Aqeeld, A.; Abidie, A. Geohazards assessment of the karstified limestone cliffs for safe urban constructions, Sohag, West Nile Valley, Egypt. *J. Afr. Earth Sci.* **2020**, *161*, 103671. [CrossRef]
35. Shah, A.A.; bin Yassin, A.M.H.E.; bin Haji Irwan, M.I.I. Is pull-apart basin tectonic model feasible for the formation of Kashmir basin, NW Himalaya. *Scientia Bruneiana.* **2017**, *16*(1). [CrossRef]
36. Nkodia, H.M.D-V.; Miyouna, T.; Delvaux, D.; Boudzoumou, F. Flower structures in sandstones of the Paleozoic Inkisi Group (Brazzaville, Republic of Congo): Evidence for two major strike-slip fault systems and geodynamic implications. *South Afr. J. Geol.* **2020**, *123*(4), 531–550. [CrossRef]
37. Baharizan, F.Z.; Ismail, M.S. The brittleness and ductility of shale from Setap shale, Miri, Sarawak. *IOP Conf. Ser.: Earth Environ. Sci.* **2022**, *1003*, 012012. [CrossRef]
38. Abdel Zaher, M.; Elbarbary, S.; El-Shahat, A.; Mesbah, H.; Embaby, A. Geothermal resources in Egypt integrated with GIS-based analysis. *J. Volcanol. Geotherm. Res.* **2018**, *365*, 1–12. [CrossRef]
39. Abdel Zaher, M.; Elbarbary, S. Investigation of Geothermal resources in Egypt using geophysical data. In Proceedings of the World Geothermal Congress, 2020+1, Reykjavik, Iceland, 24–27 October 2021.
40. Theilen-Willige, B. Remote sensing and geographic information system (GIS) contribution to the inventory and investigation of dikes in Egypt. *Mediterr. J. Basic Appl. Sci.* **2023**, *7*(3), 60–84. [CrossRef]

41. Theilen-Willige, B. Overview of circular structures of various origins and sizes in Egypt as a contribution to natural hazard data mining based on remote sensing data and geoinformation systems (GIS) analysis. *Prevention and Treatment of Natural Disasters.* **2023**, *2*(2), 7–19. [CrossRef]
42. Salama, A.; Hussein, H.; Abdelazim, M.; El-Nader Iman, A. Reinvestigation of the 1978 Gilf El Kebir earthquake, Egypt. *NRIAG J. Astron. Geophys.* **2023**, *12*(1), 143–148. [CrossRef]
43. Sherif, M.A.; Badreldin, H. Present-day stress field in Egypt based on a comprehensive and updated earthquake focal mechanisms catalog. *Pure Appl. Geophys.* **2019**, *176*, 4729–4760. [CrossRef]
44. PreventionWeb, the global knowledge-sharing platform for disaster risk reduction and resilience. Available online: https://www.preventionweb.net/